Experiencing Dust Storms in the Seas of the Old World

Emin Özsoy

Institute of Marine Sciences, METU, Erdemli, Mersin 33130 Turkey

2nd Training Course on WMO SDS-WAS
(Satellite and ground observation and modelling of atmospheric dust)
Antalya, 21-25 November 2011

Experiencing dust storms at Erdemli, Northern Levantine coast – Griffin et al. 2007

sampling tower

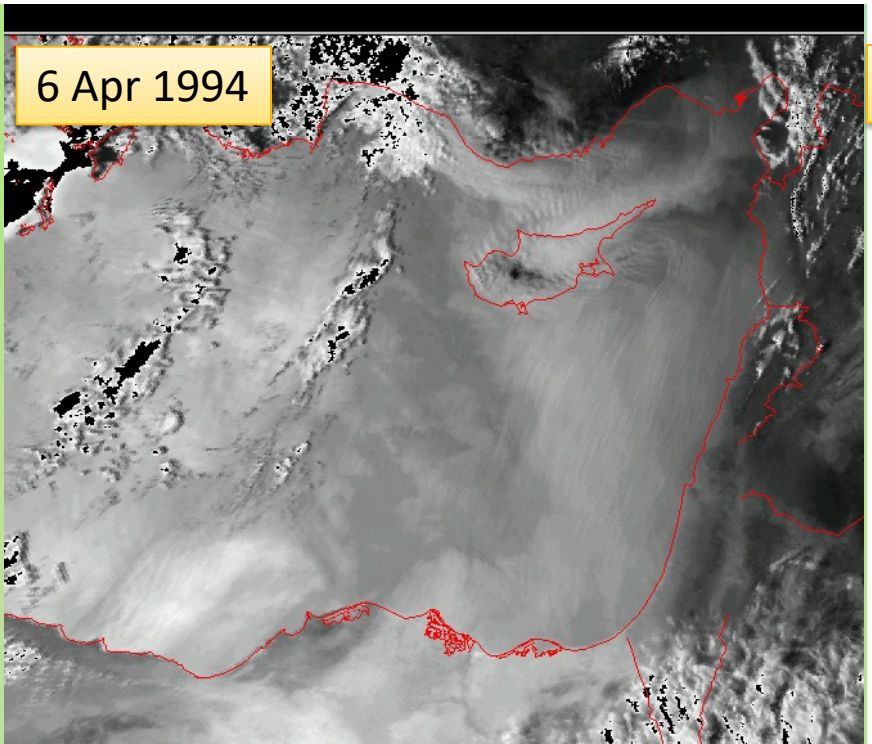

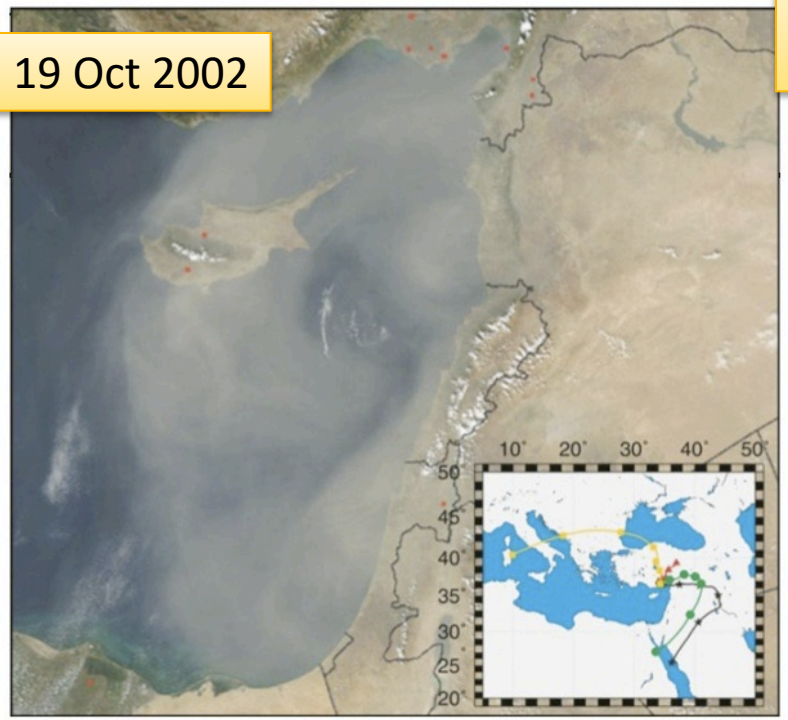

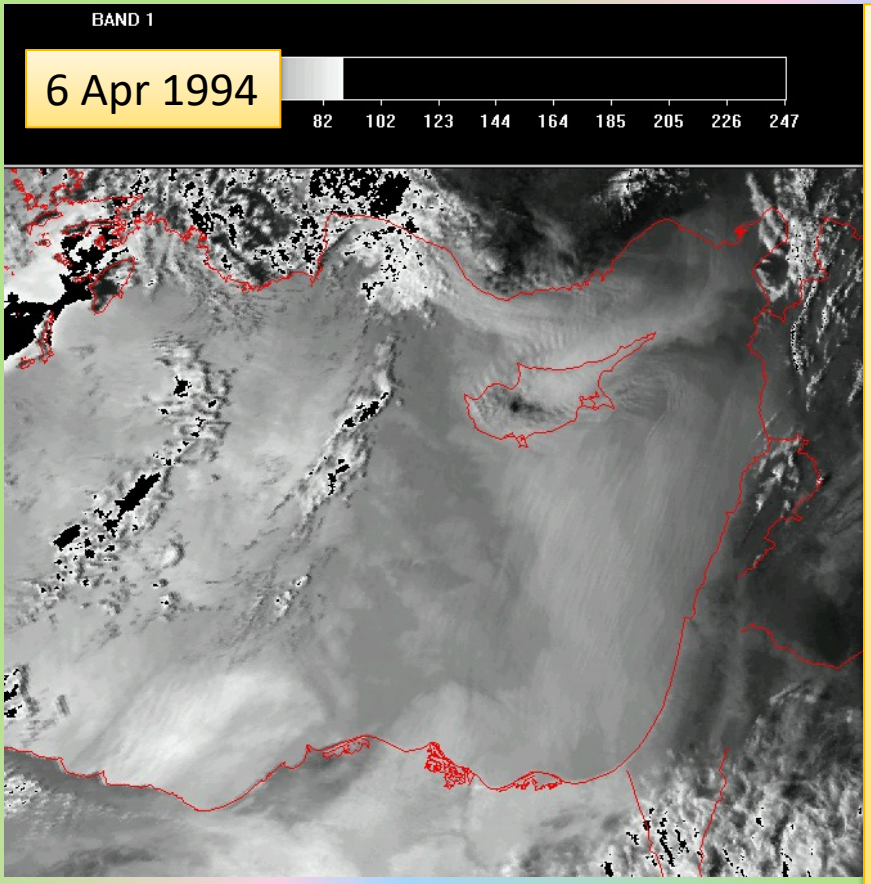

Dust storm of April 1994
Motivation for Erice dust model development

Belgrade Eta model - Janjic et al. (1993, 1994)
WorldLab Erice – 1991
INM Tunisia 1993

Nickovic and Dobricic (1996)
Nickovic (1996)
Papadopoulos et al. (1997)
Nickovic (2001)
Özsoy et al. (2001)
Nickovic et al. (2004)
Nickovic (2005)
Perez et al. (2006a, 2006b)

Skylab astronaut picture
STS049-092-071 Sandstorm,
Southern Algeria and Niger May 1992

Hemispheric scale dust events

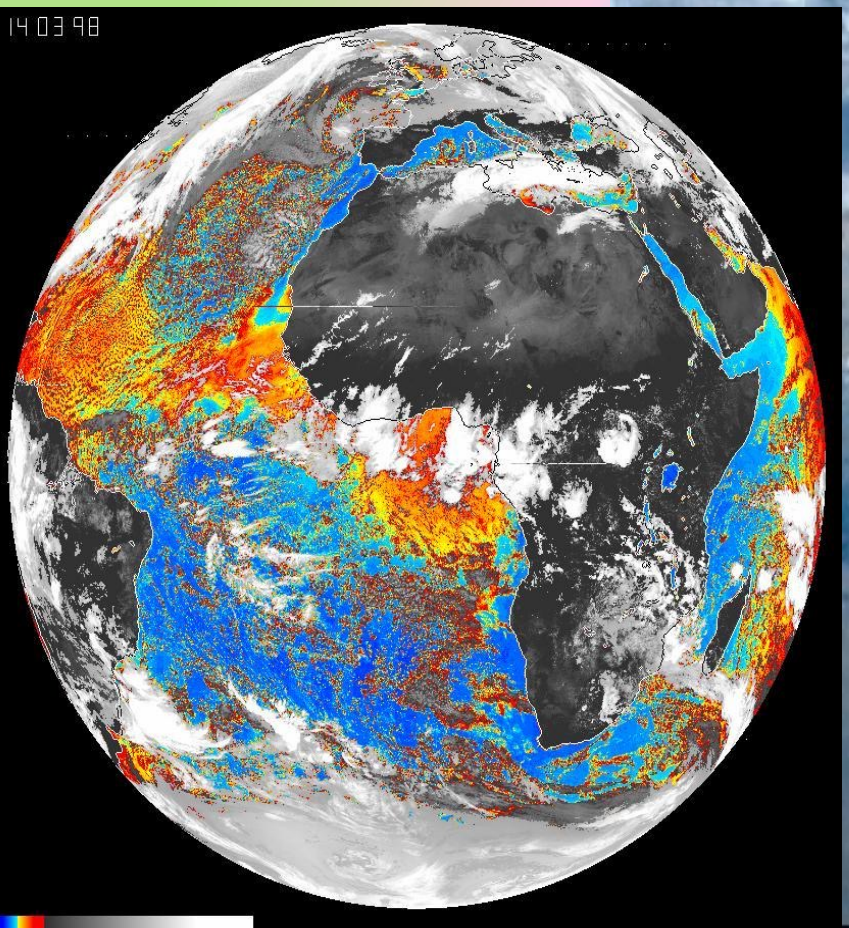

Dust sources
AI – aerosol index
Goudie et al., 2001

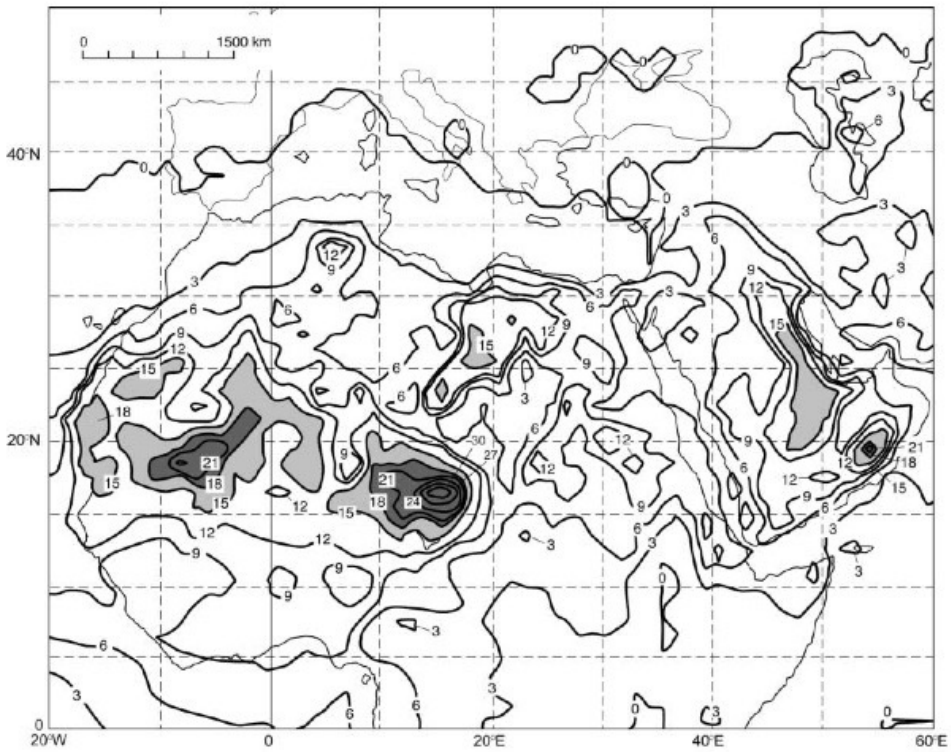

Fig. 1. Annual mean Aerosol Index for the Sahara, derived from TOMS.

Europe and Atlantic

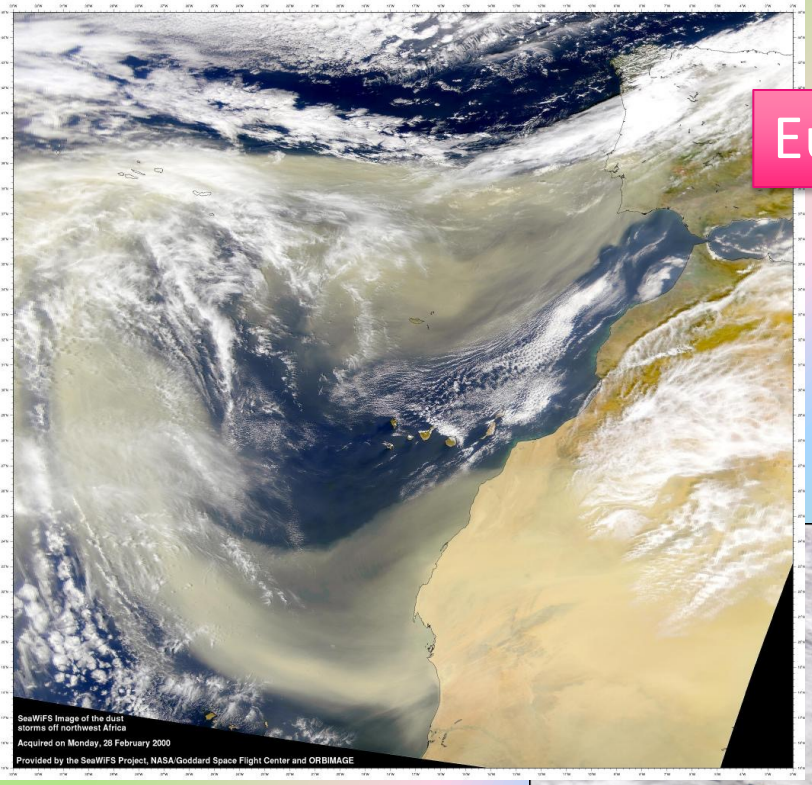

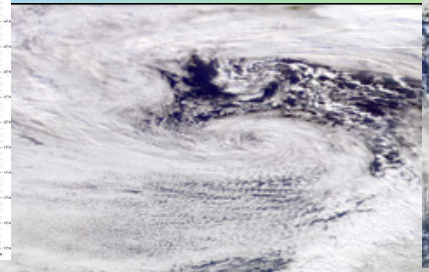

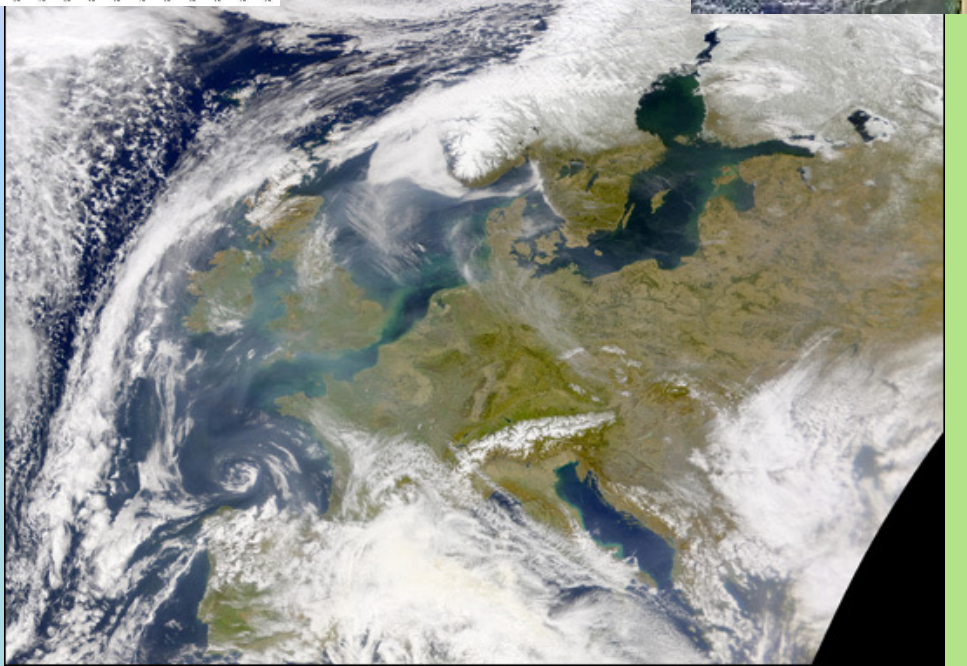

Mediterranean

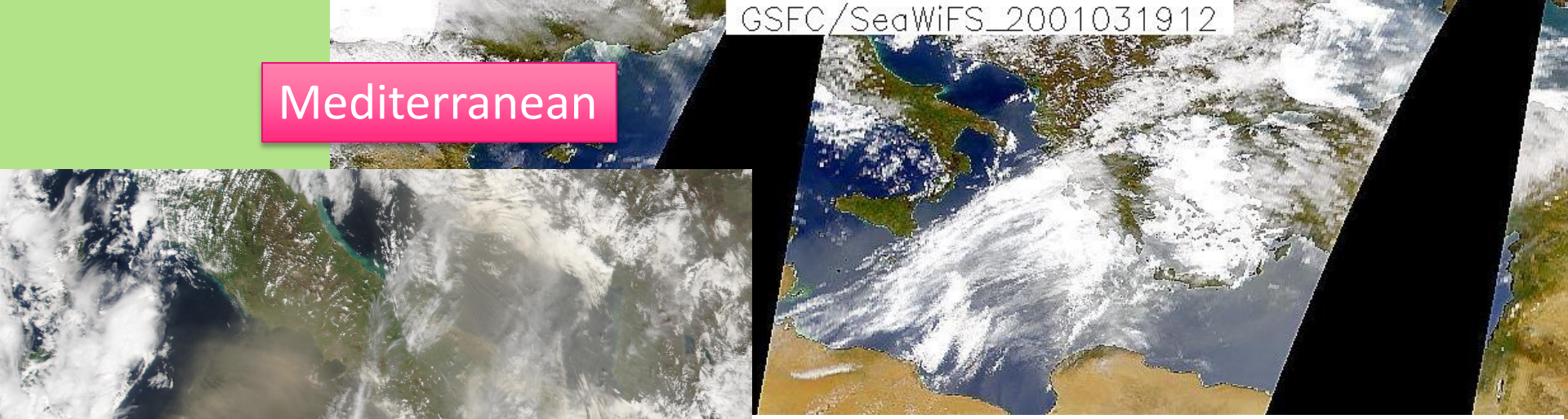

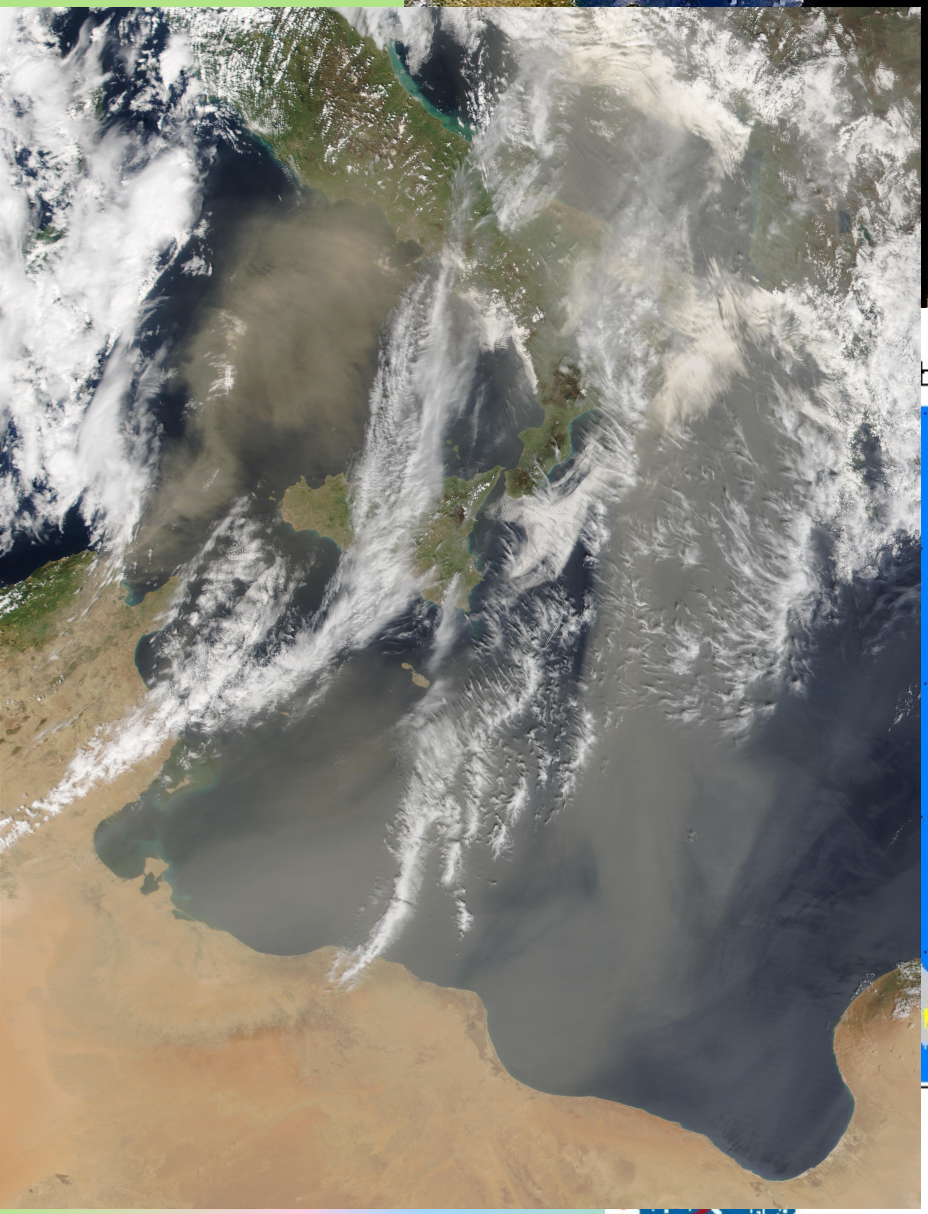

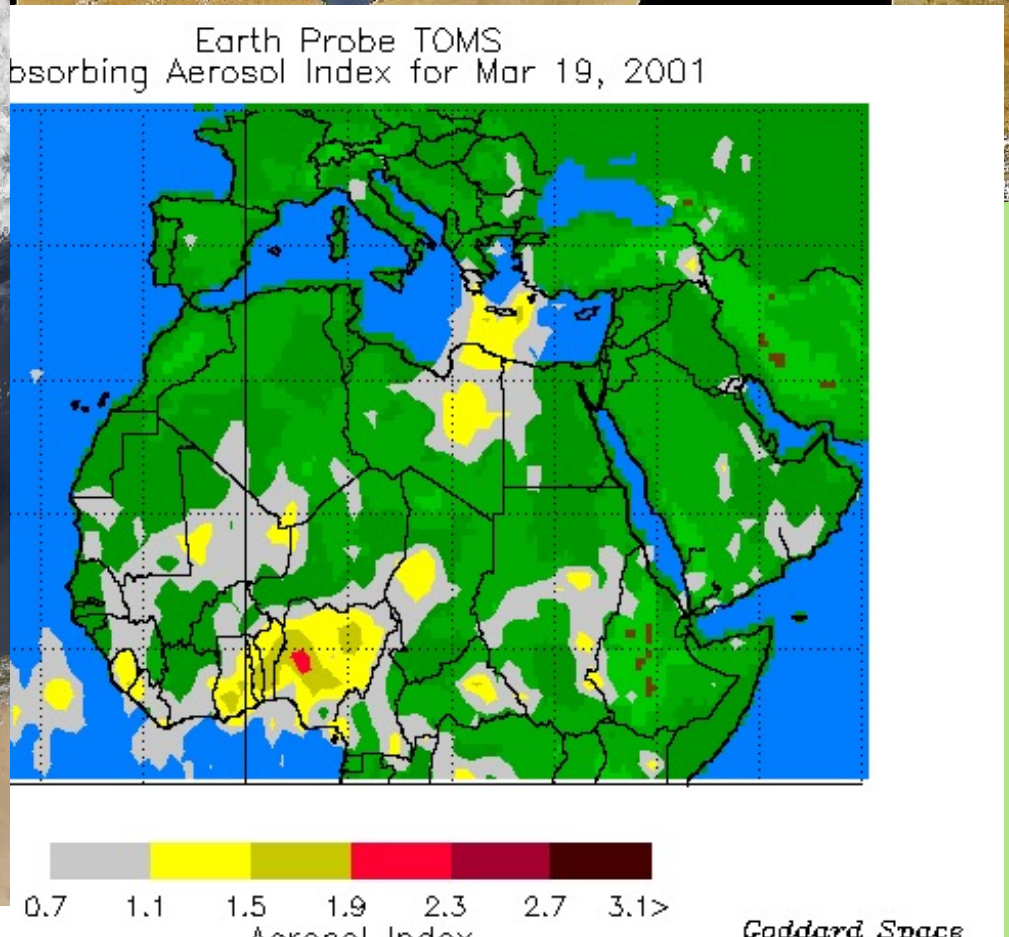

Airborne dust (brown haze) over the Caribbean Sea. This dust originated in the Sahara Desert of western Africa where it was lifted and carried off the coast by strong winds.

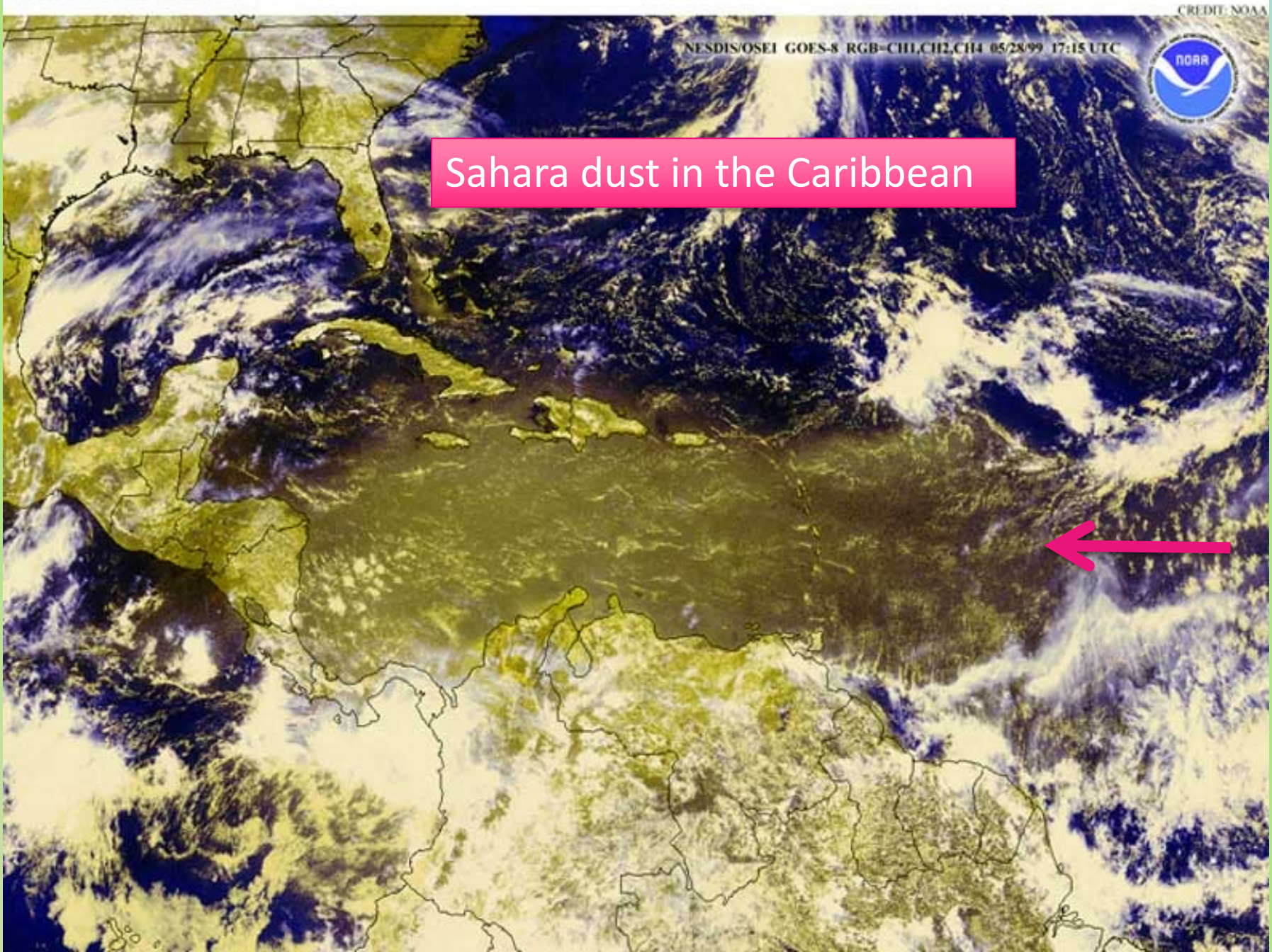

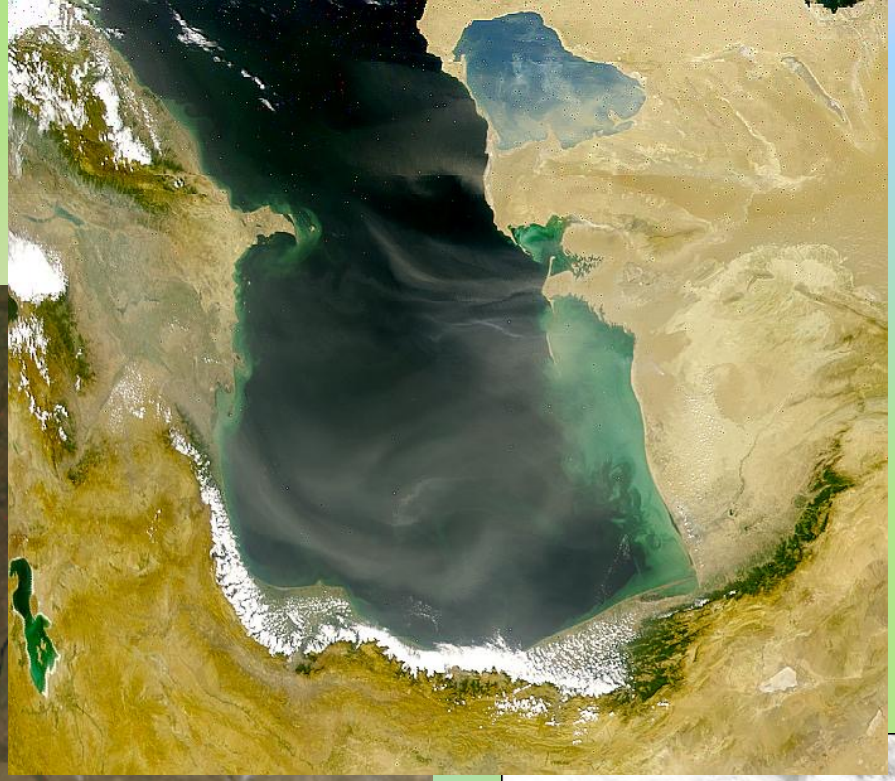

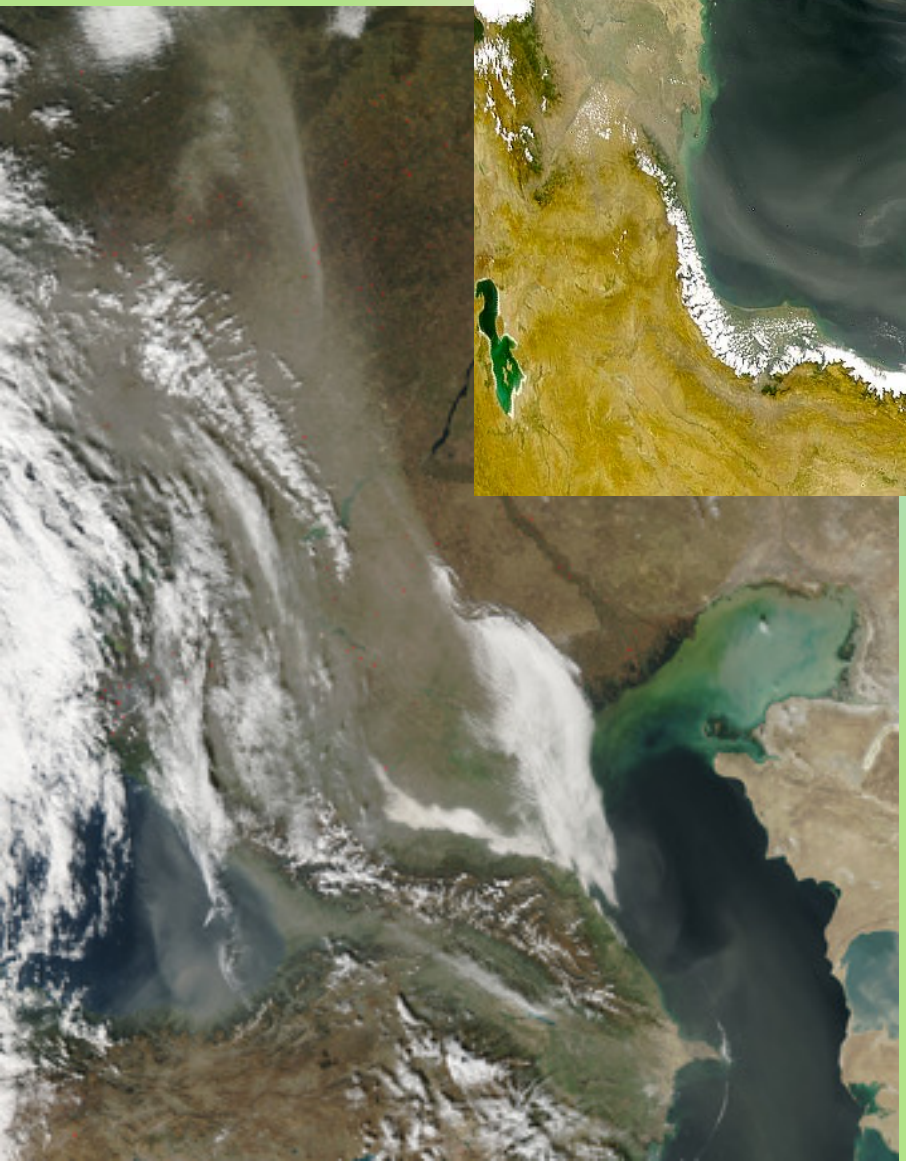

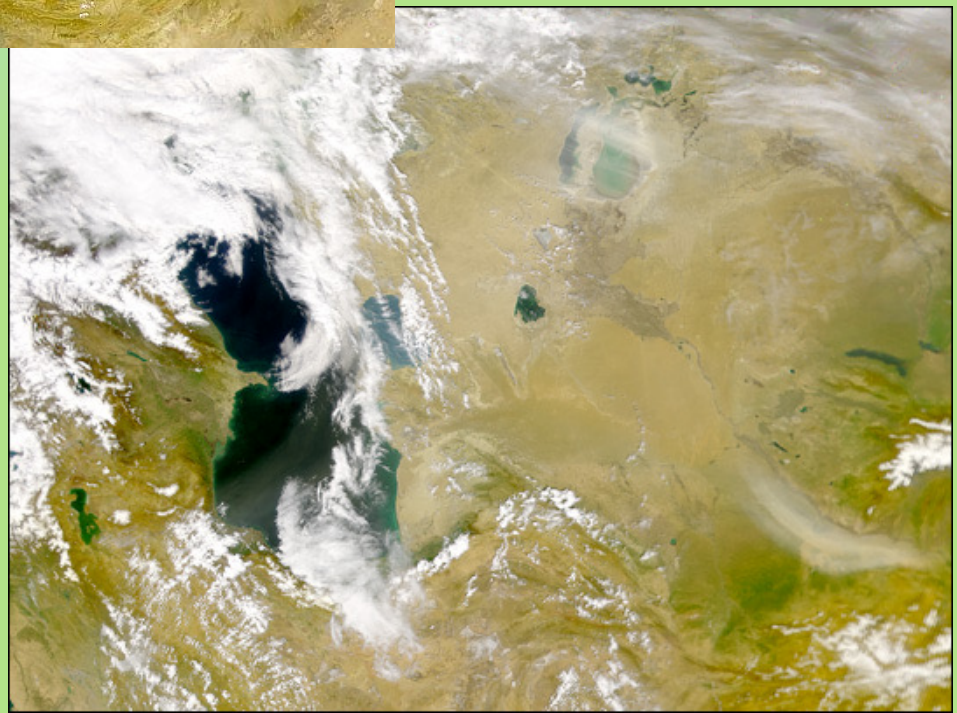

Black Sea
Caspian Sea
Central Asia

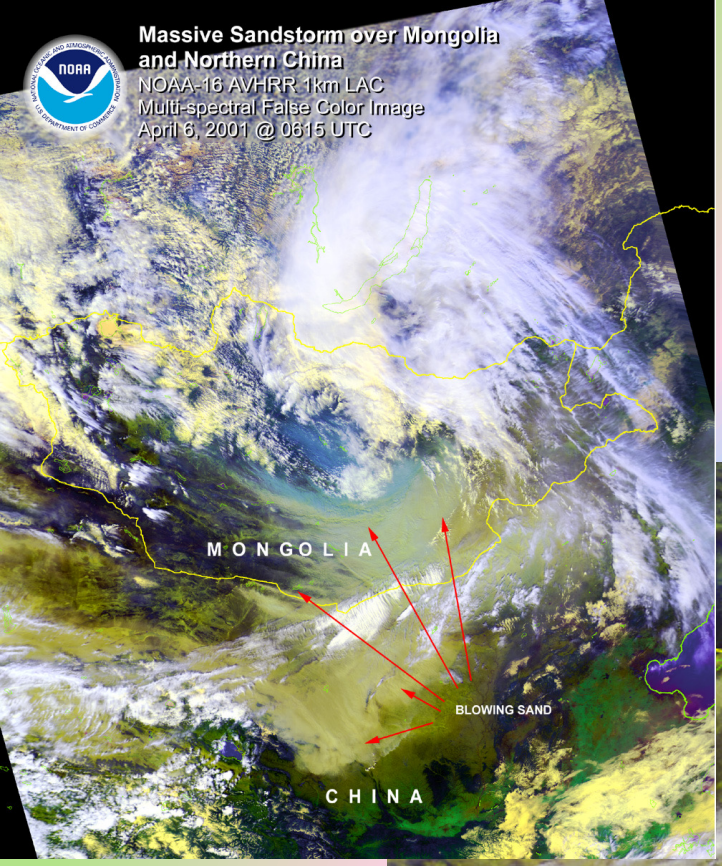
Massive Sandstorm over Mongolia
and Northern China
NOAA-16 AVHRR 1km LAC
Multi-spectral False Color Image
April 6, 2001 @ 0615 UTC
MONGOLIA
BLOWING SAND
CHINA

East Asia

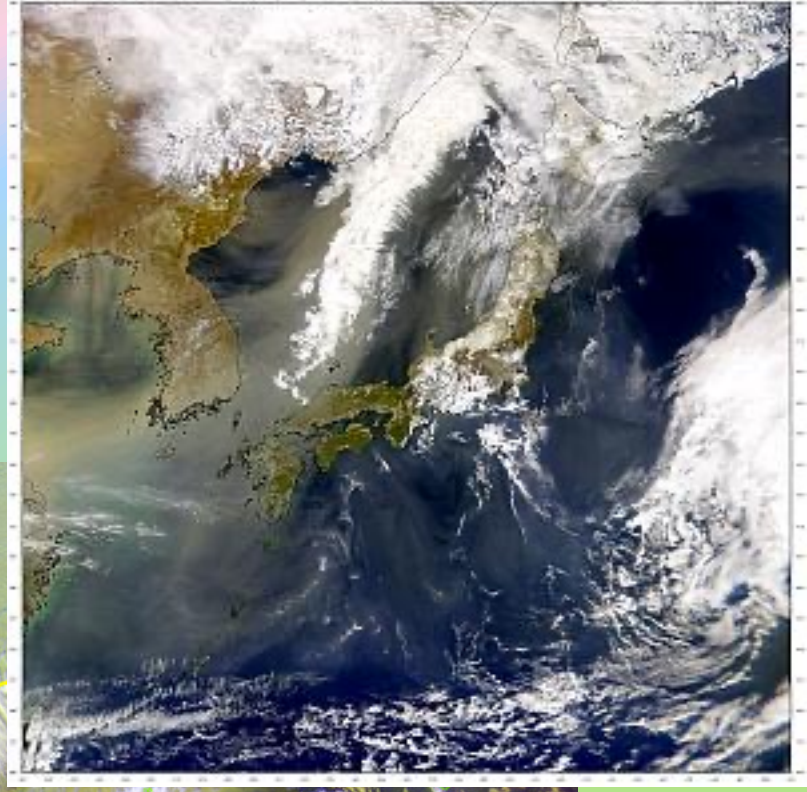

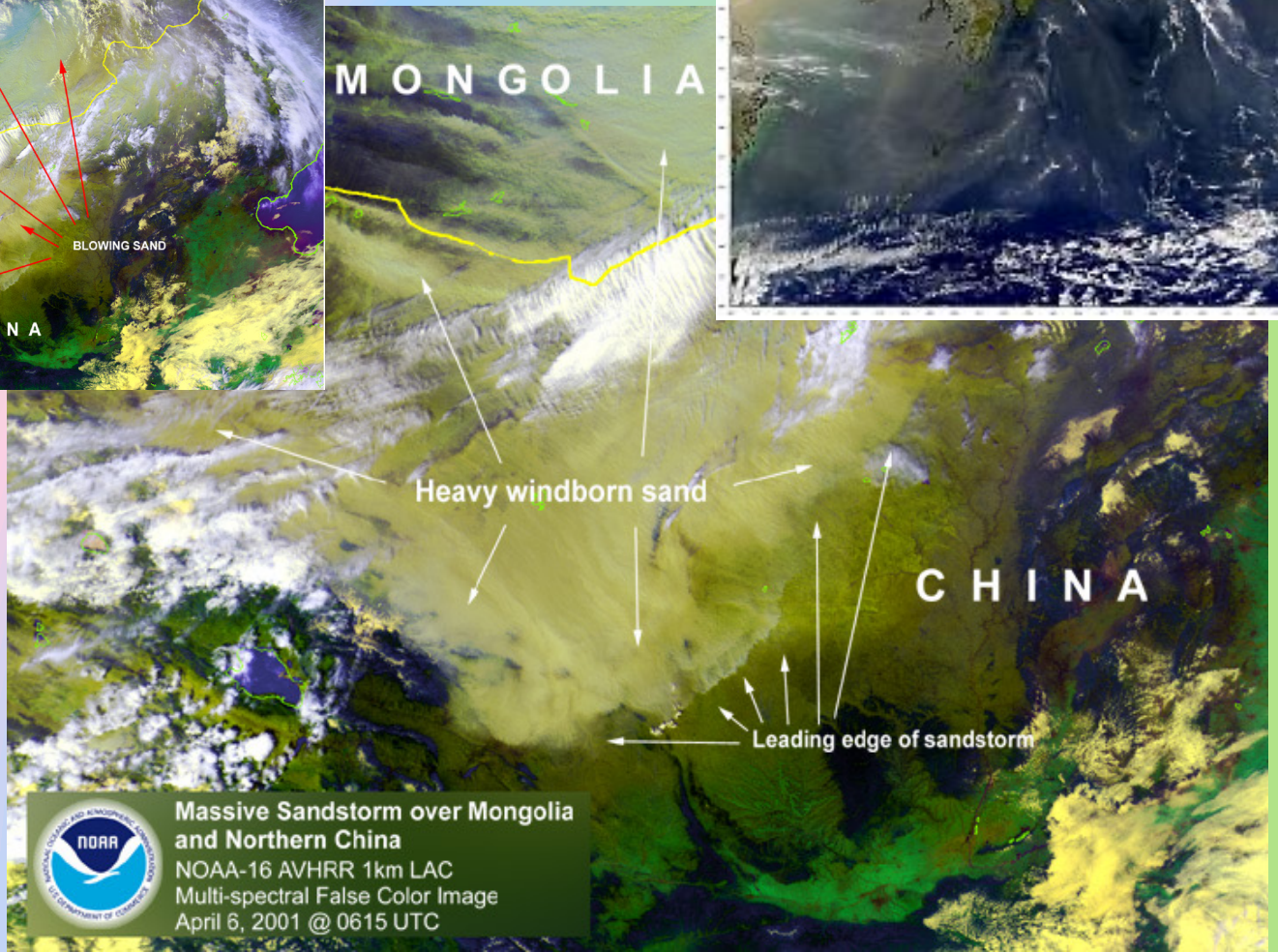
MONGOLIA
Heavy windborn sand
CHINA
Leading edge of sandstorm
Massive Sandstorm over Mongolia
and Northern China
NOAA-16 AVHRR 1km LAC
Multi-spectral False Color Image
April 6, 2001 @ 0615 UTC

Example of a hemispheric dust event: qerosol index for 4-14 Apr 2001
Taklamakan desert -> China -> Pacific Ocean -> USA -> Atlantic Ocean
Maher, B. A. Aeolian Research 2011.

From East Asia to Atlantic around the world

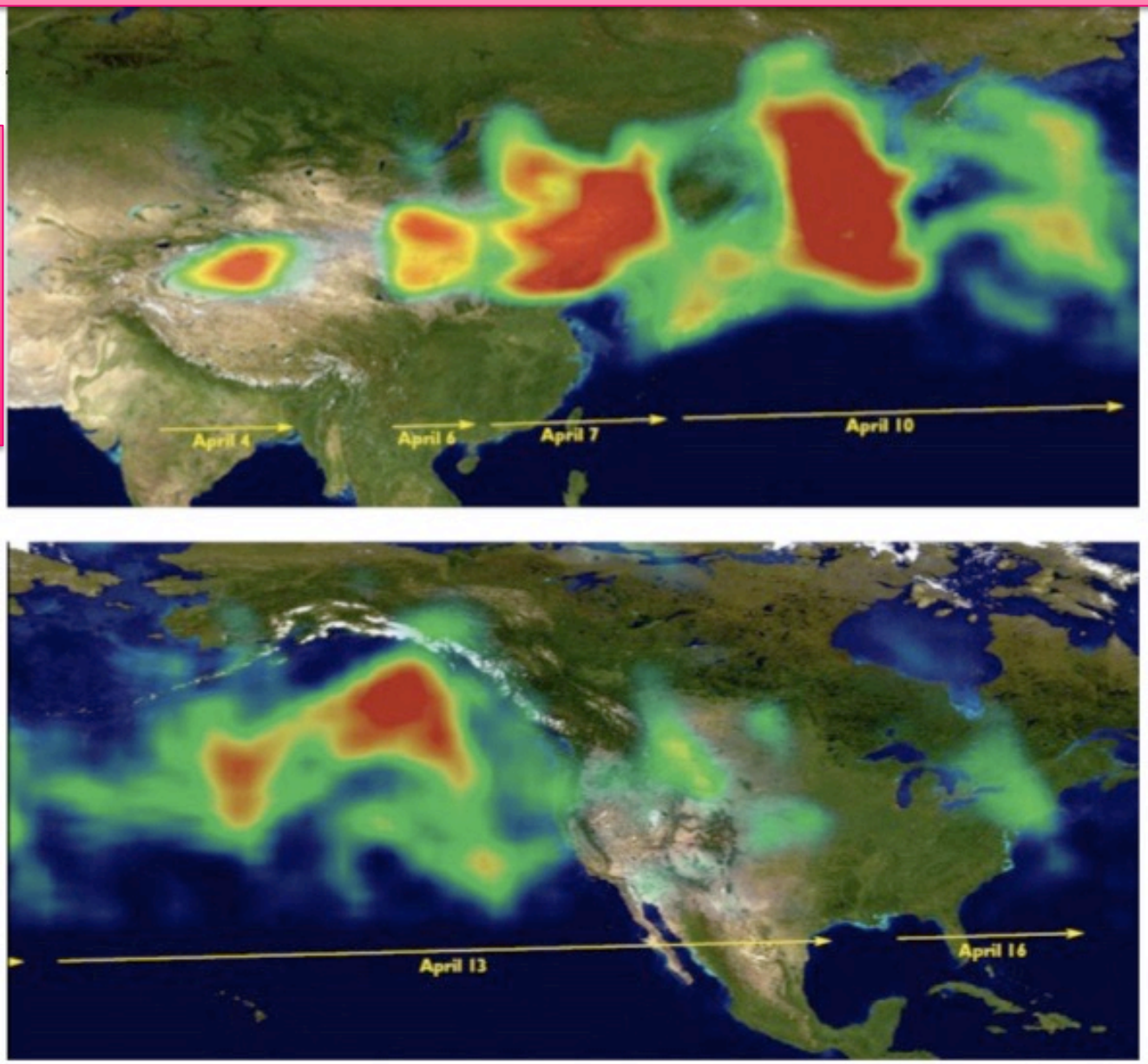

MEDITERRANEAN / ATLANTIC DUST STORM OF APRIL 1994
strong NAO+ phase event

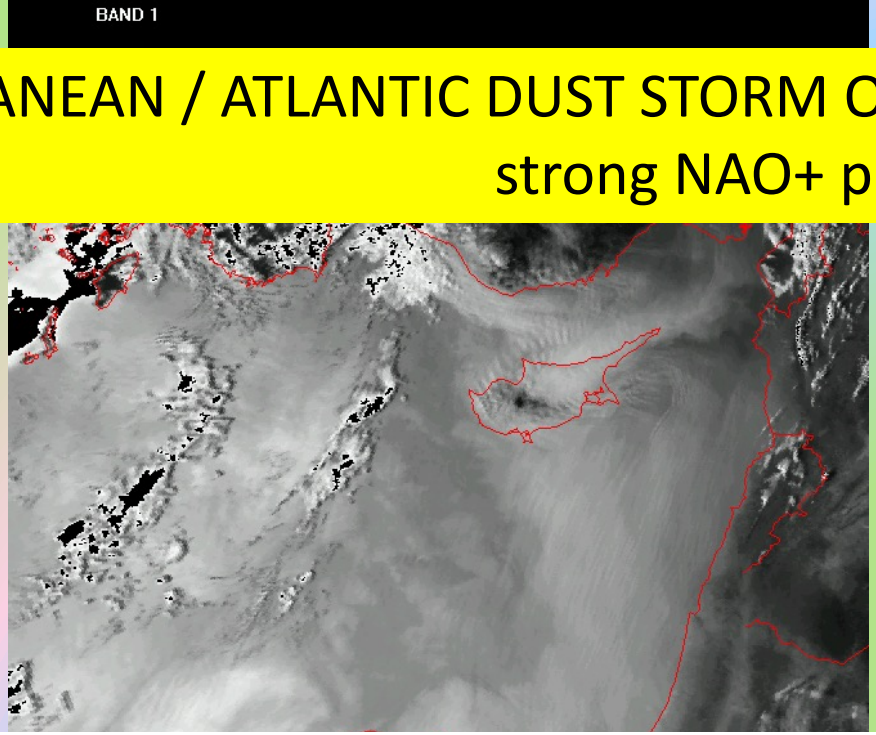

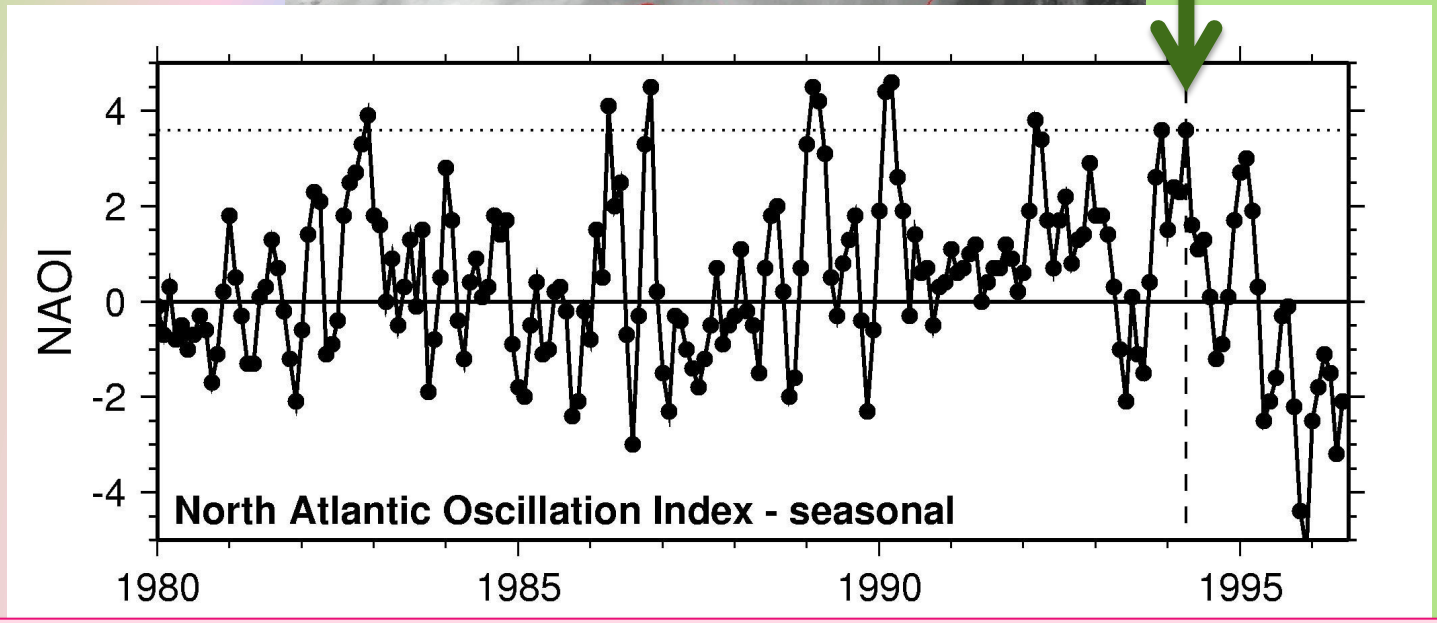

Özsoy, E., Kubilay, N., Nickovic, S. and C. Moulin, J. Geophys. Res., 106, 18,439 - 18,460, 2001.

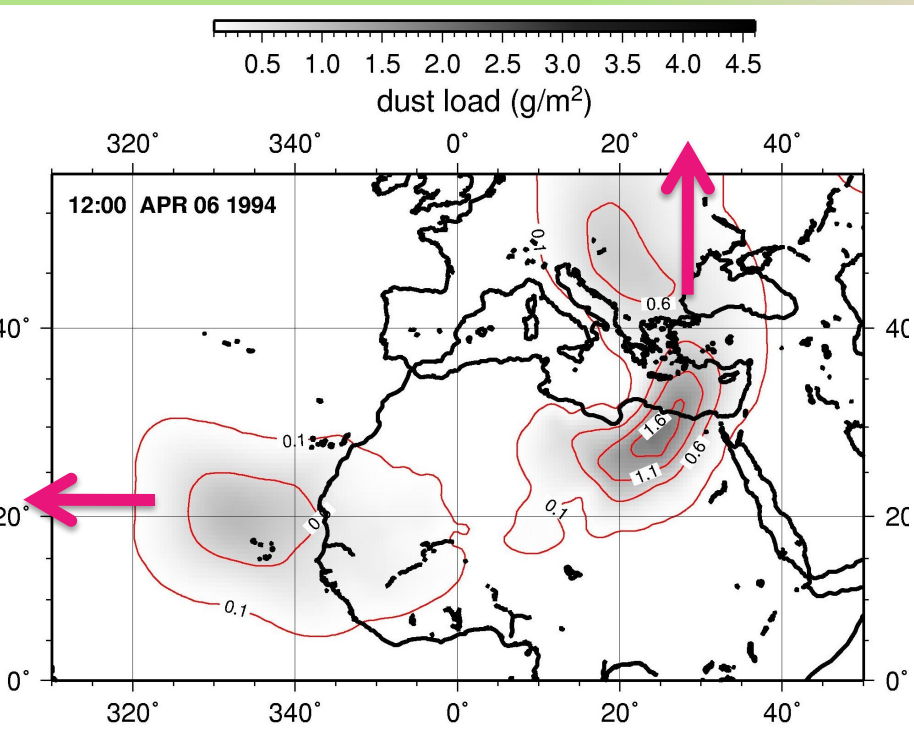

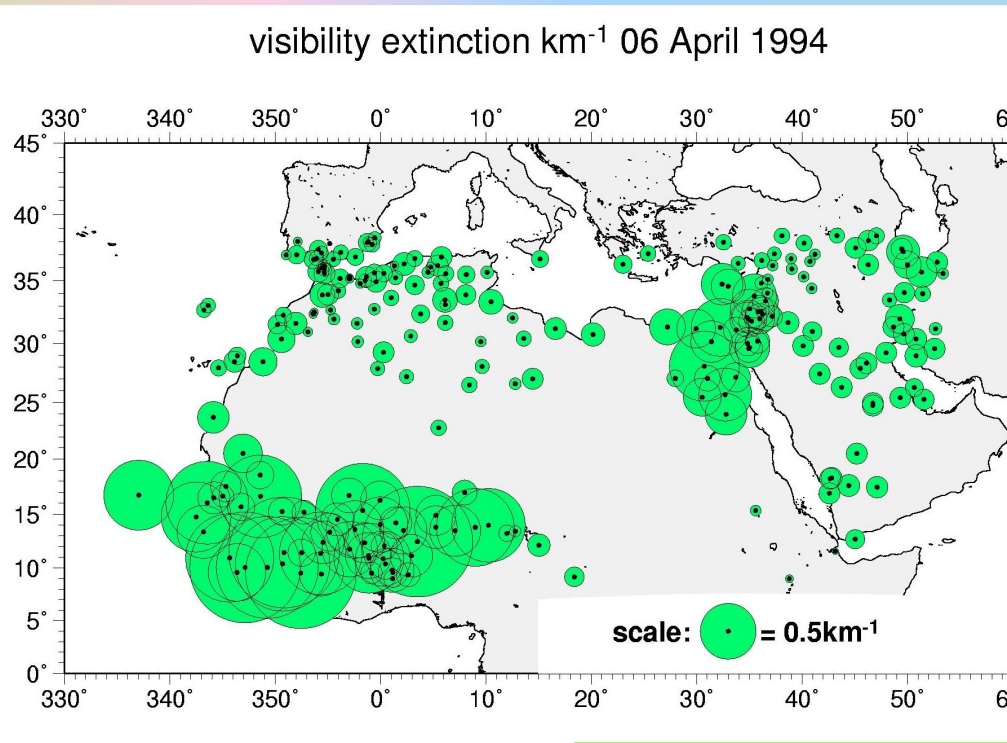

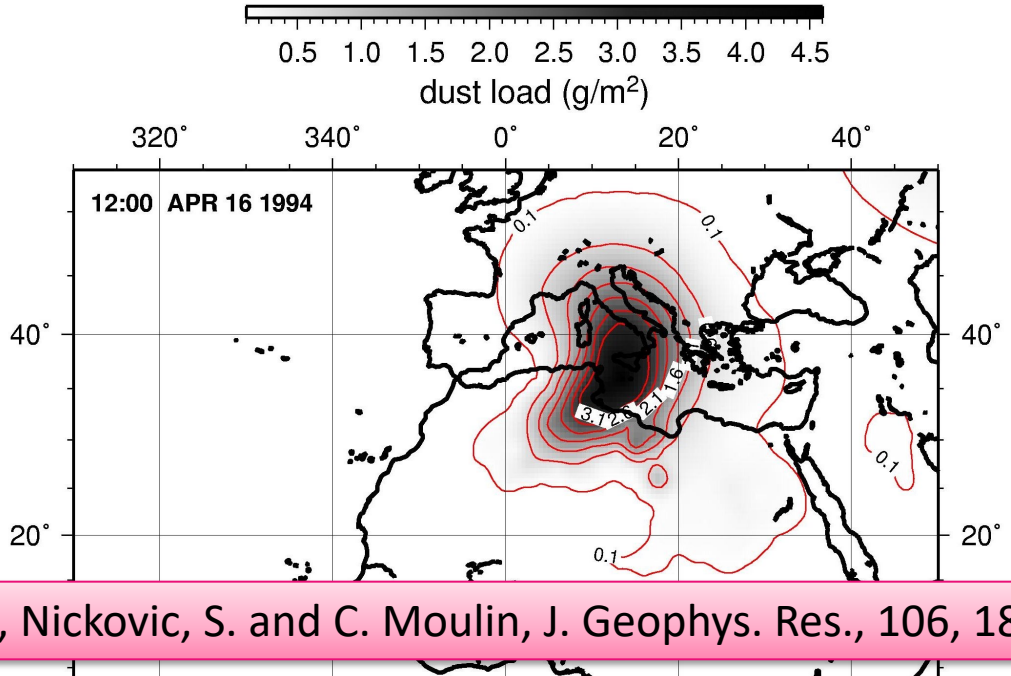

Özsoy, E., Kubilay, N., Nickovic, S. and C. Moulin, J. Geophys. Res., 106, 18,439 - 18,460, 2001.

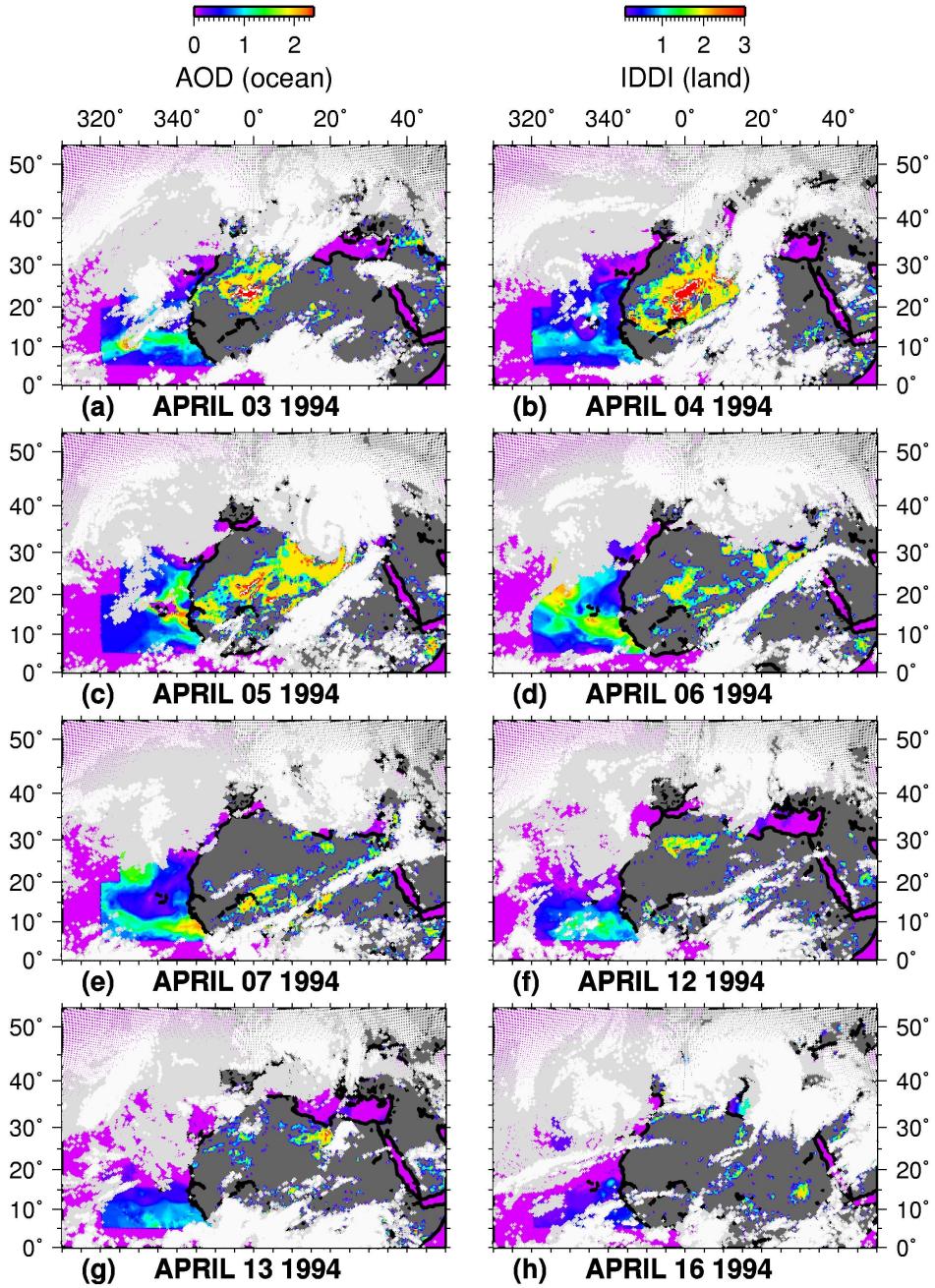

1994 April dust storm affecting Atlantic Ocean and the Mediterranean
Özsoy, *et al.*, 2001

- high positive phase NAO) I
- Atlantic blocking anticyclone
- polar front and subtropical jets interaction
- Sahara subsidence
- Sahara cyclogenesis
- simultaneous incursion of Sahara
  - Atlantic: easterlies
  - Mediterranean: growing cyclone

-repeated series of dust transport events 3-5 Apr 94 and 15-17 Apr 94.

maximum ground concentrations:
- Erdemli, Turkey: 1.6 mg/m^3
- Barbados 0.28 mg/m^3
  (highest reported in 30-years, Li *et al.*, 1996).

MARCH 31 - APRIL 13 1994

Upper air jet interactions

Polar front jet versus subtropical jet

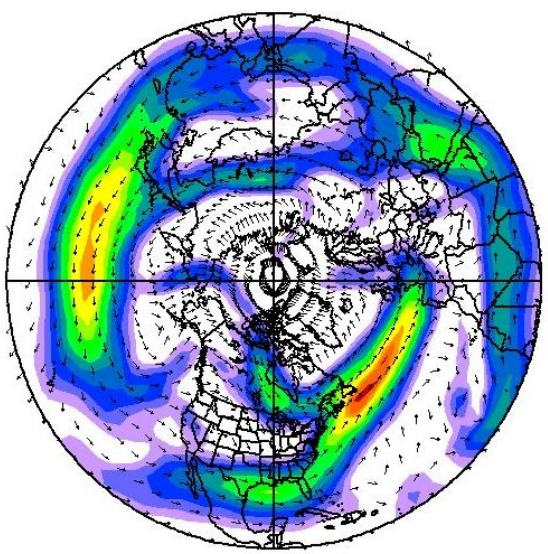

250mb WINDS (m/s) 02-DAY MEAN FOR:
Thu MAR 31 1994 – Fri APR 01 1994

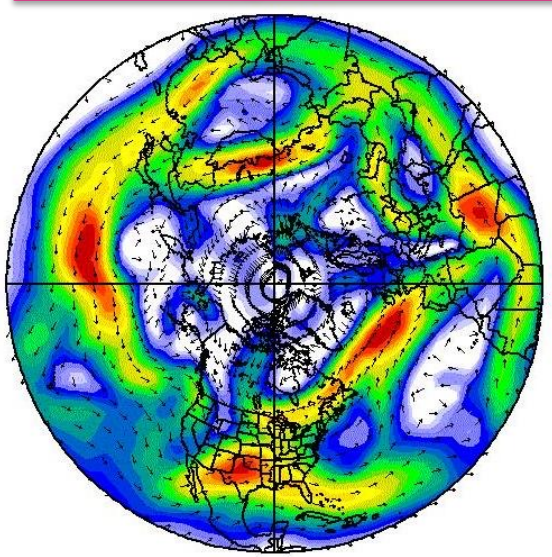

250mb WINDS (m/s) 02-DAY MEAN FOR:
Mon APR 04 1994 – Tue APR 05 1994

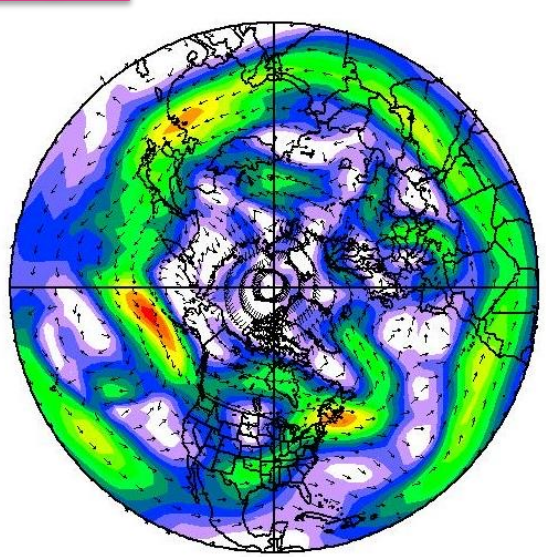

250mb WINDS (m/s) 02-DAY MEAN FOR:
Tue APR 12 1994 – Wed APR 13 1994

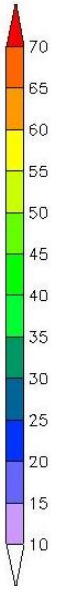

upper air jet interaction
-> Sahara cyclogenesis

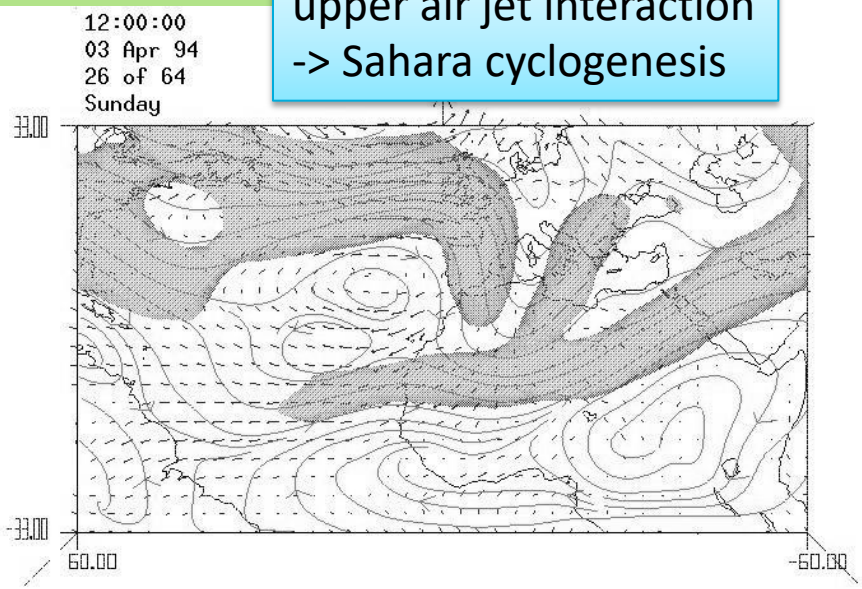

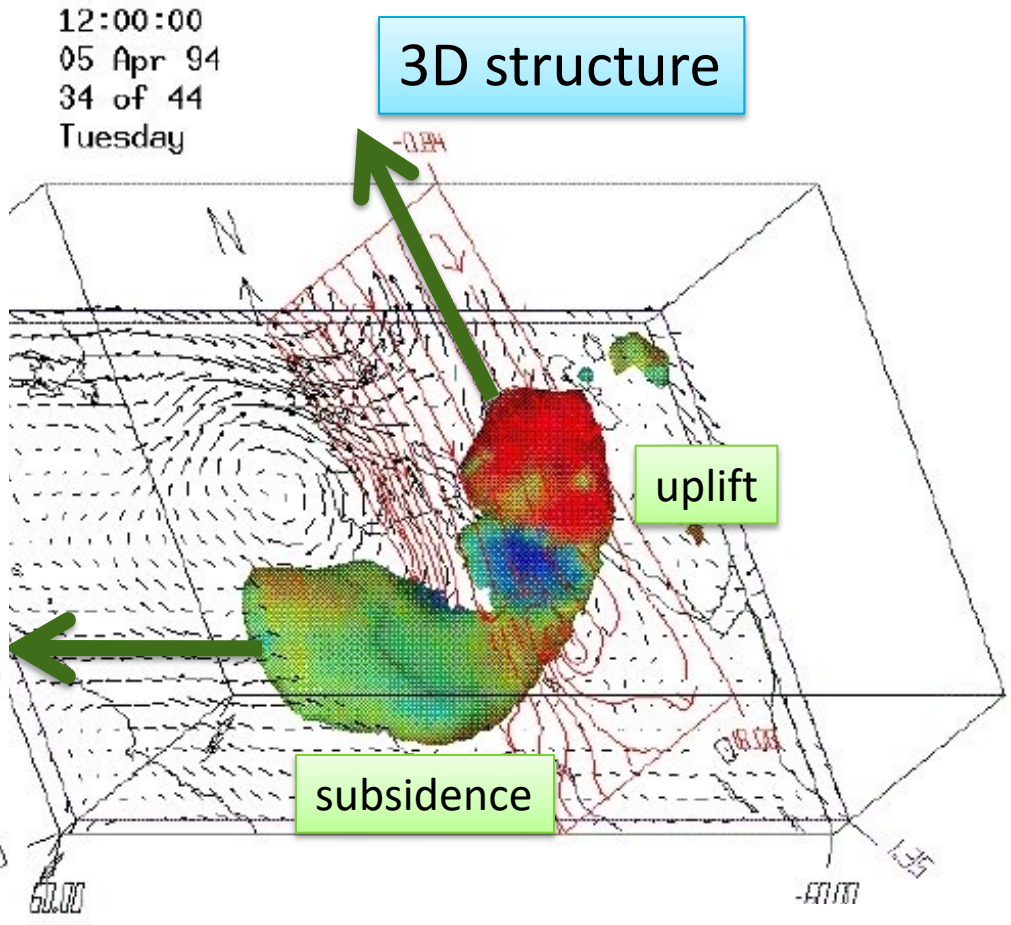

3D structure

uplift

subsidence

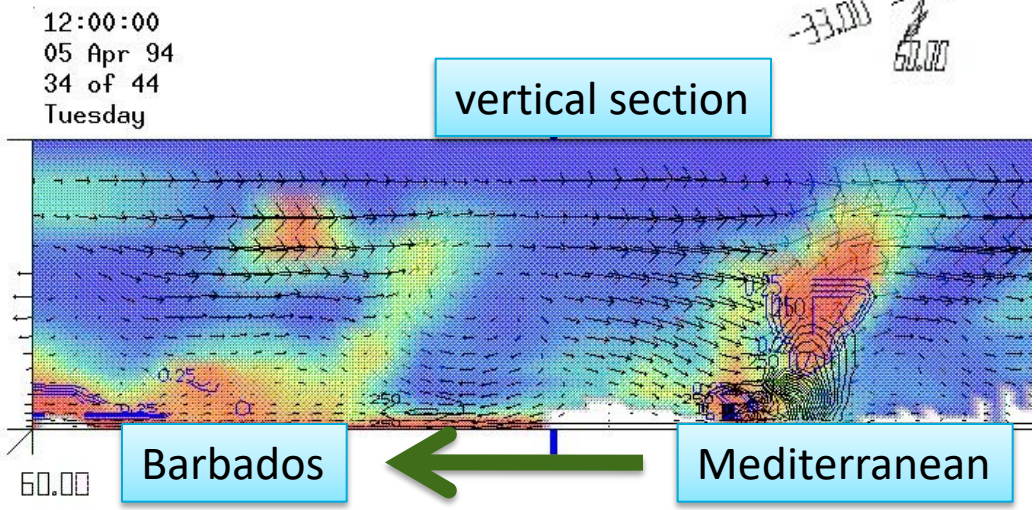

vertical section

Barbados

Mediterranean

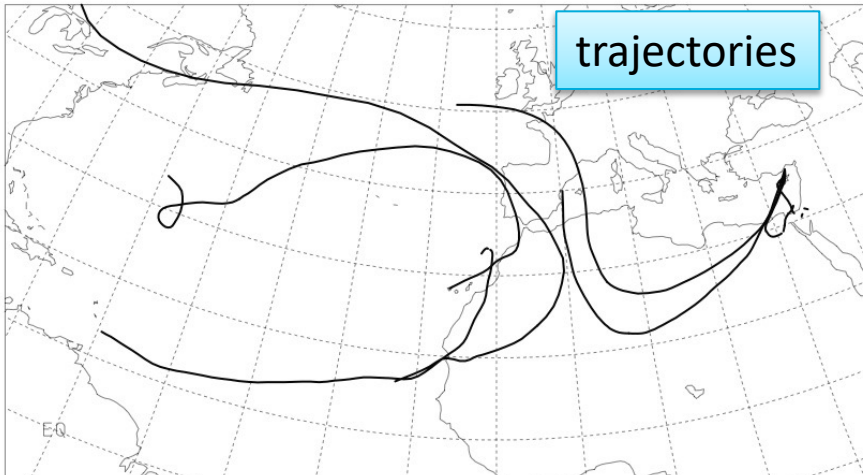

trajectories

ARAL-KUM - EU COPERNICUS PROGRAMME

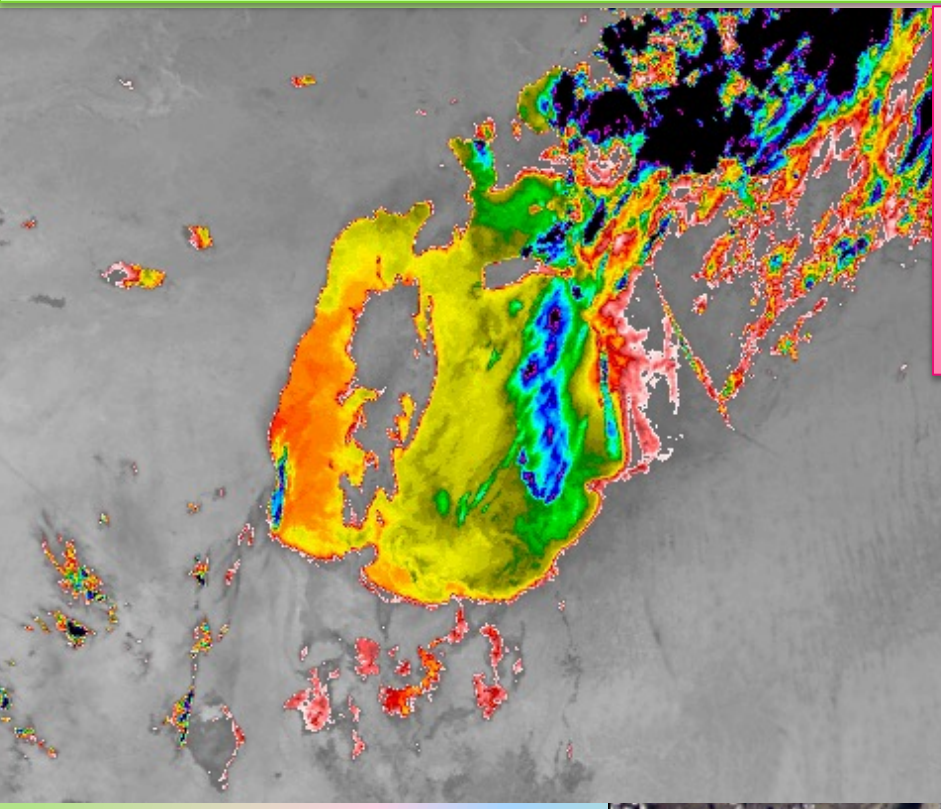

ARAL SEA dust transport

The dust, partially a result of the desiccation of the Aral Sea, has adverse effects on the local population and the socio-economic well being affecting Uzbekistan / Kazakhstan

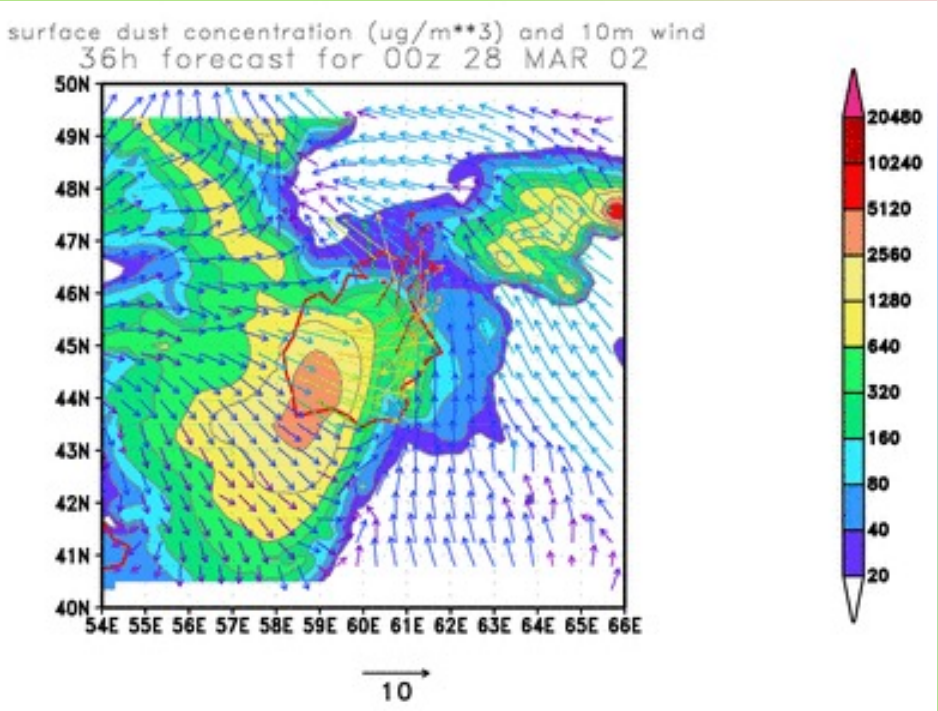

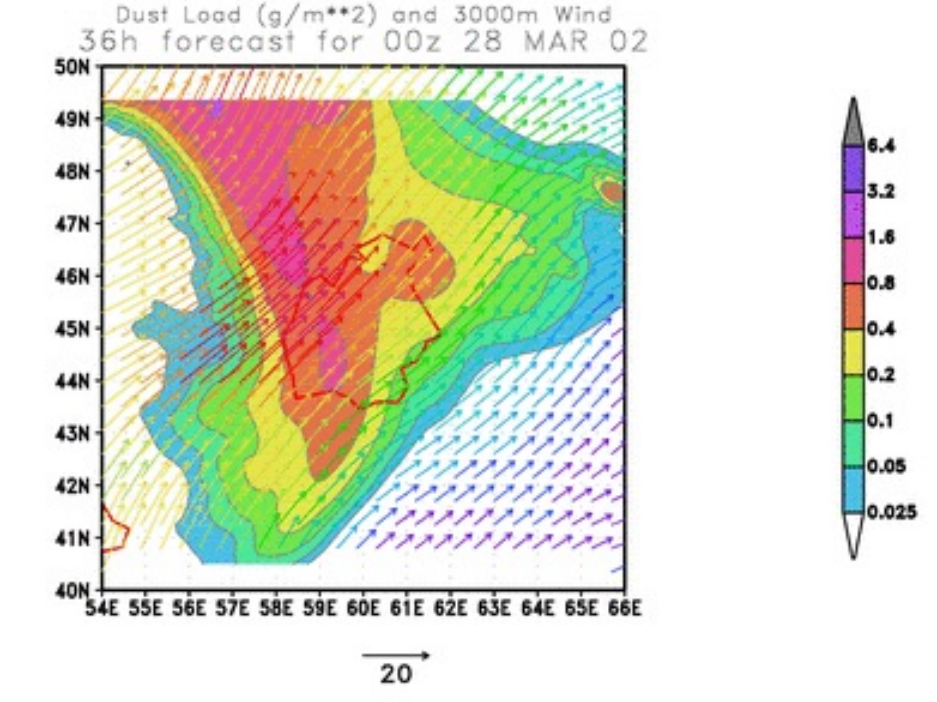

Aral Sea dust model forecasts
28 March 2002 at 00z

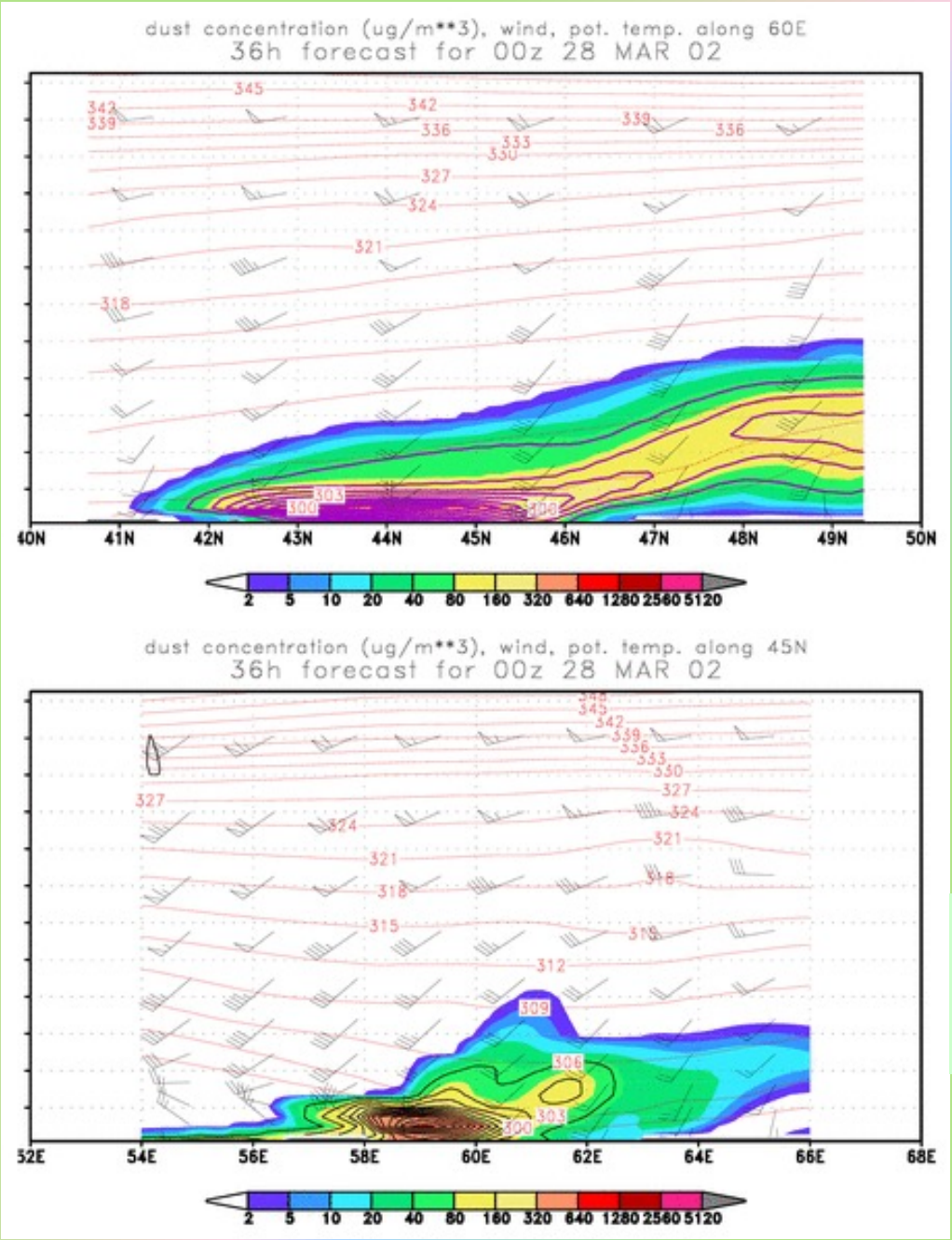

Aral Sea dust model forecasts

The dust near the Aral Sea is confined to the shallow and stable atmospheric boundary layer over the desert

this is why the dust has particularly strong ill-effects, carrying salts and fertilizers (previously used for cotton production)

(top:) south-north section along 60E, (bottom:) east-west section along 45N on 30 March 2002 at 12z.

The vertical sections of dust concentration indicate upper air injection of fine dust particles at major topographic barriers such as the Alpine and Himalayan mountain ranges.

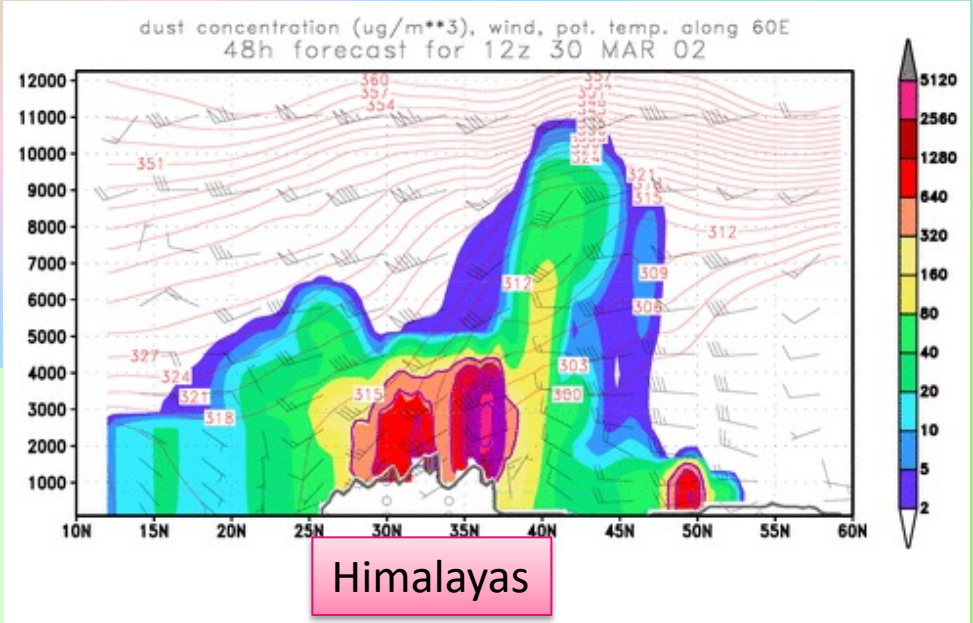

EURO-ASIAN Forecasts
Continuous dust suspension – transport - deposition

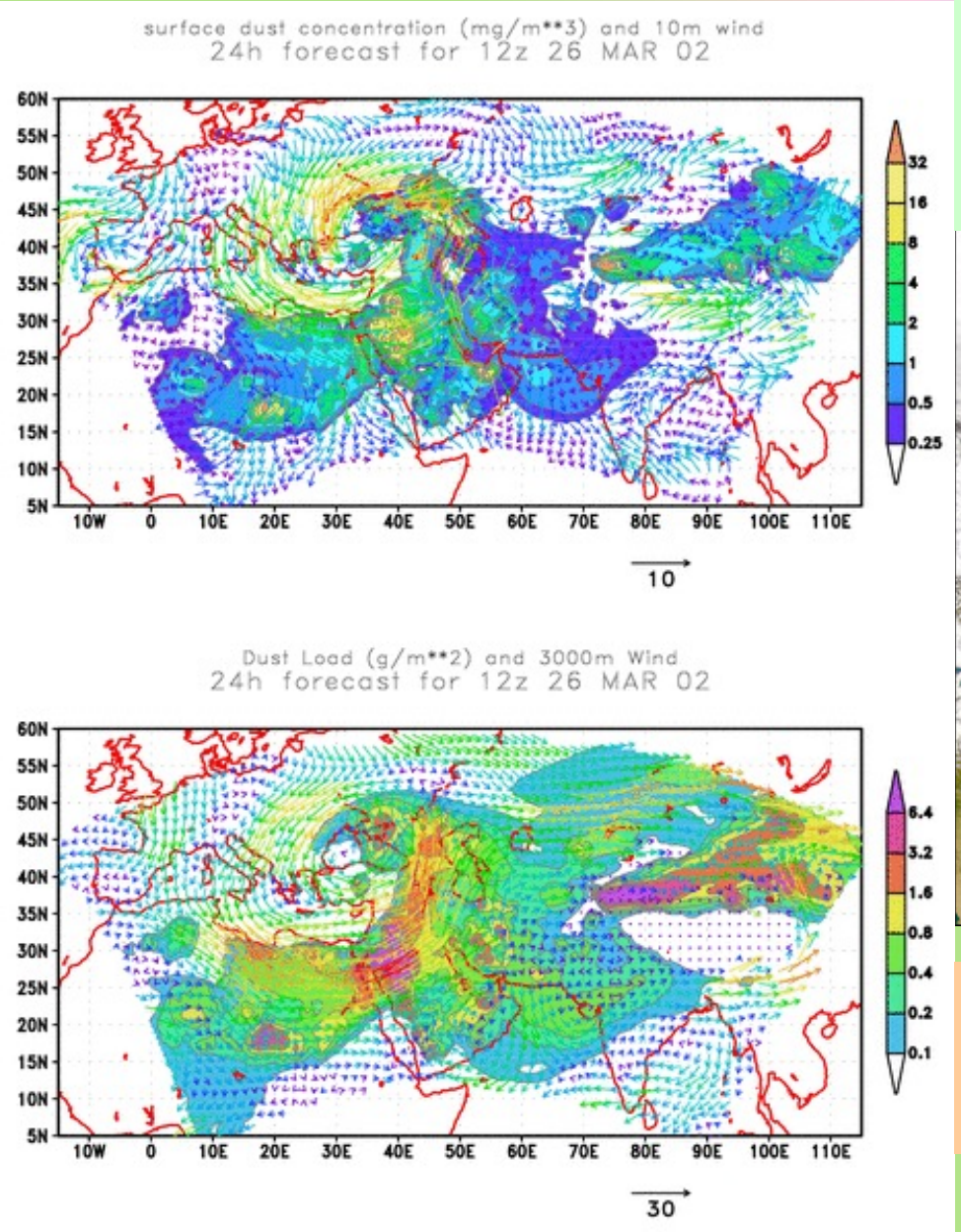

Dust storms covering three continents (Africa, Europe and Asia) and all Euro-Asian seas were identified while studying the Aral Sea dust storms.

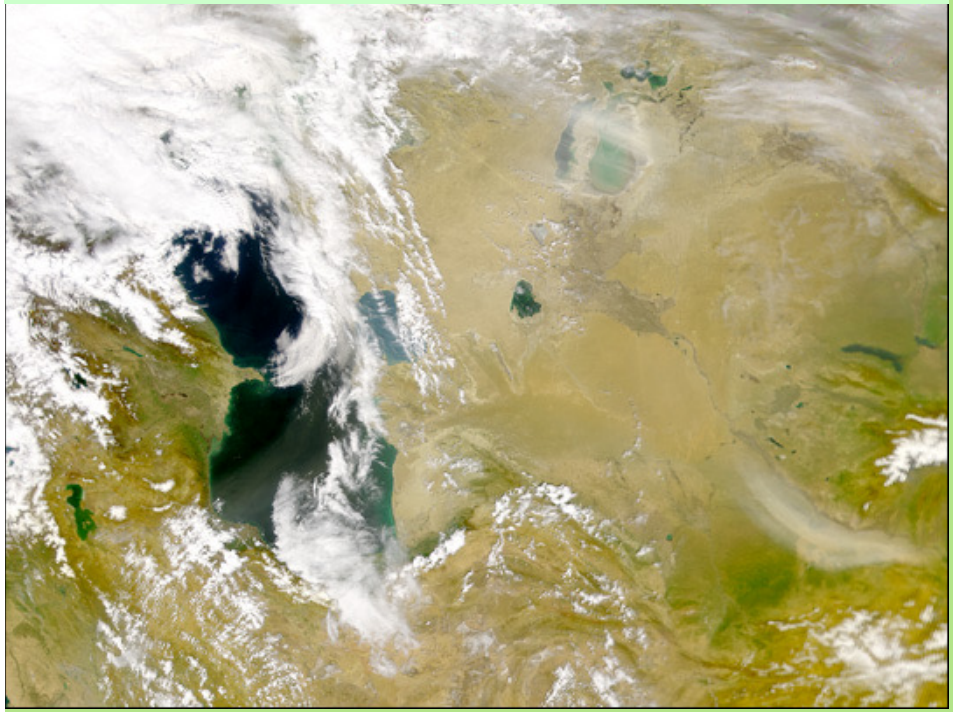

dust model forecast on 26 March 2002, 12z, and seawifs image

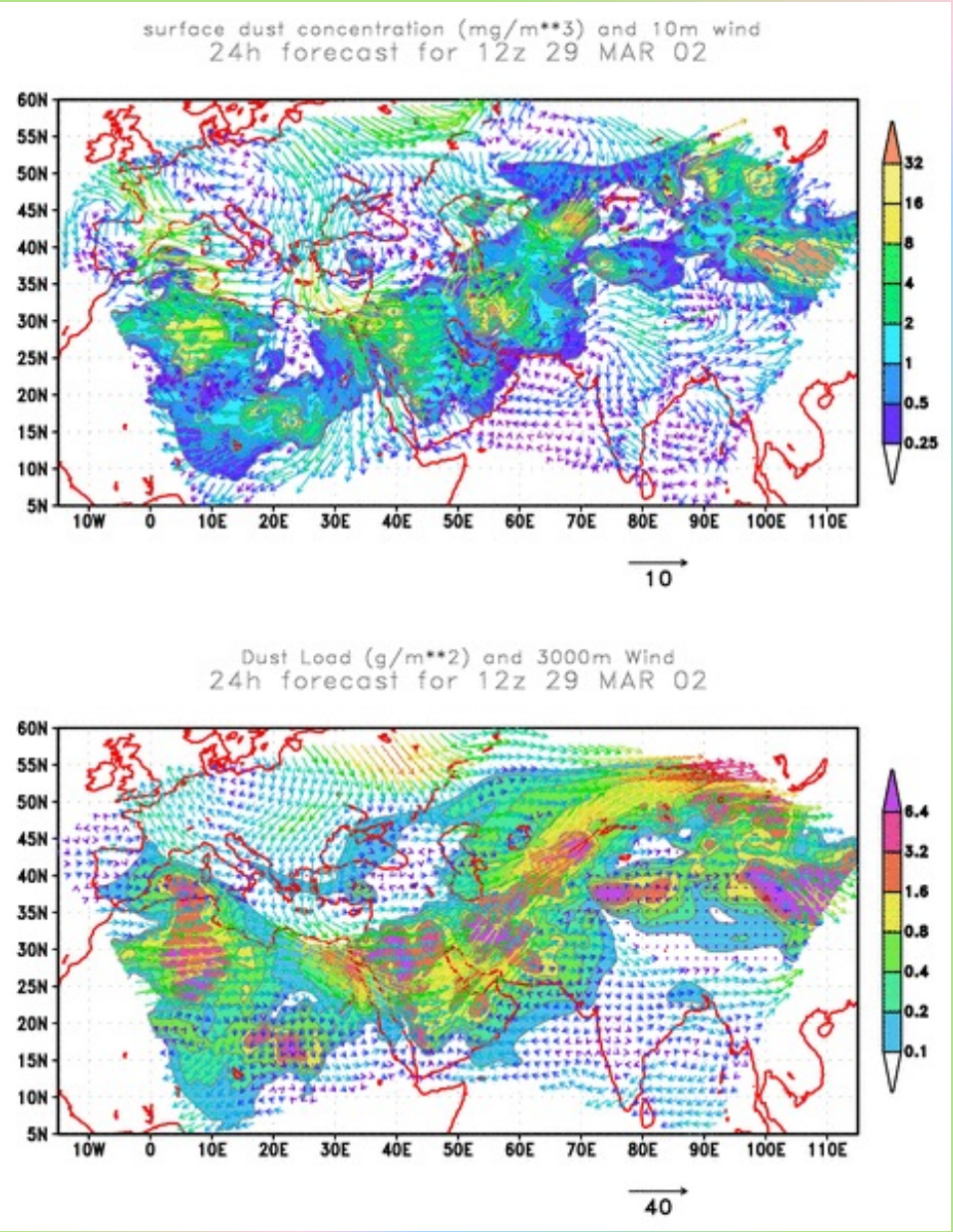

dust model forecasts on 29 March 2002, 12z, and seawifs image

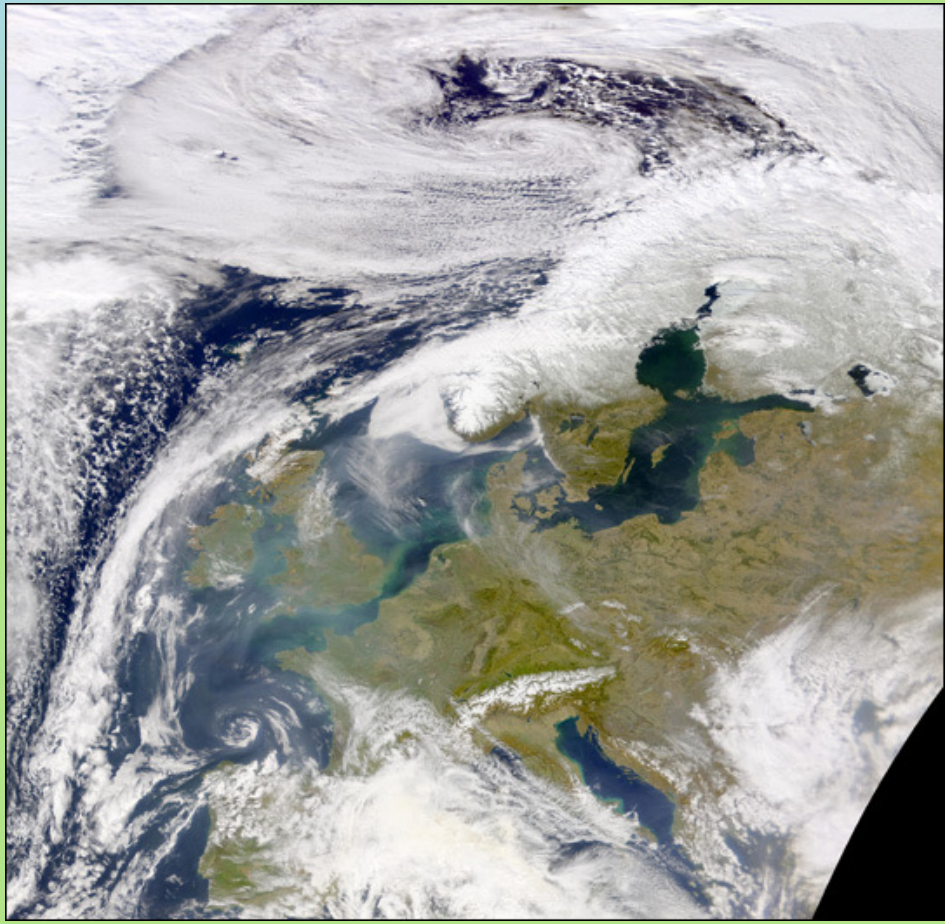

dust model forecast on
13 April 2002, 12z,
and seawifs image

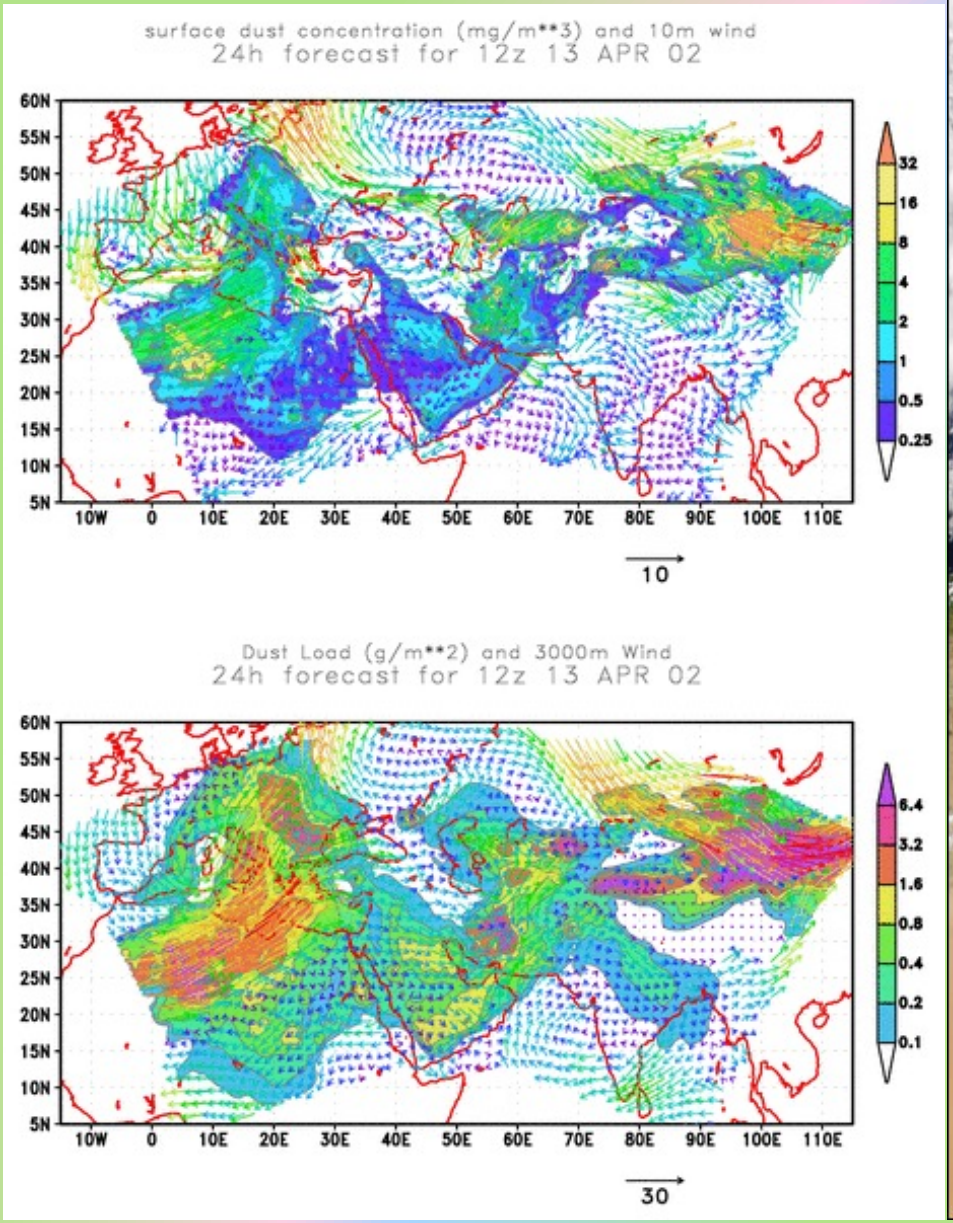

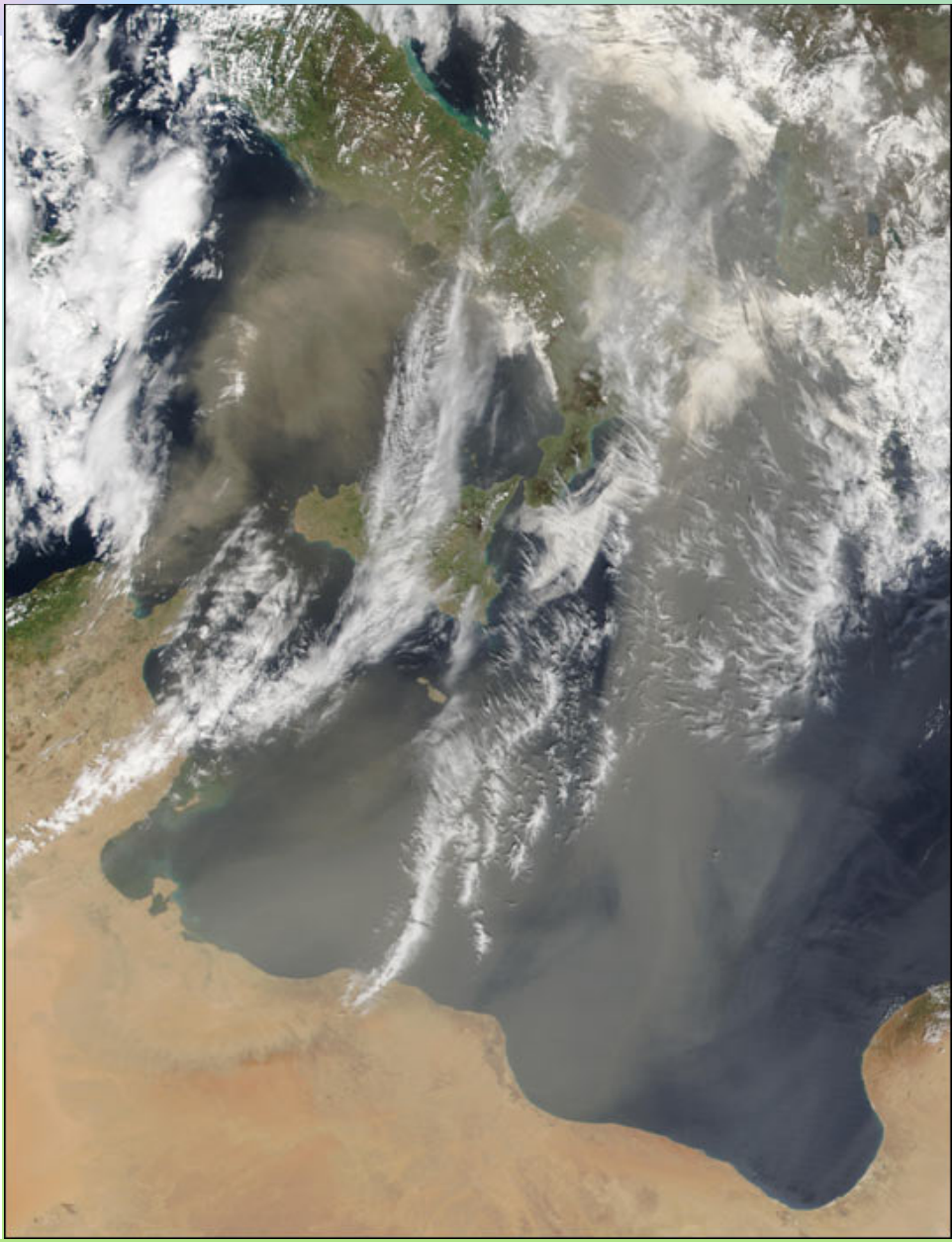

Pérez, C., Nickovic, S., Pejanovic, G., Baldasano, J. M. and E. Özsoy, J. Geophys. Res., 2009
Dust effects on radiation

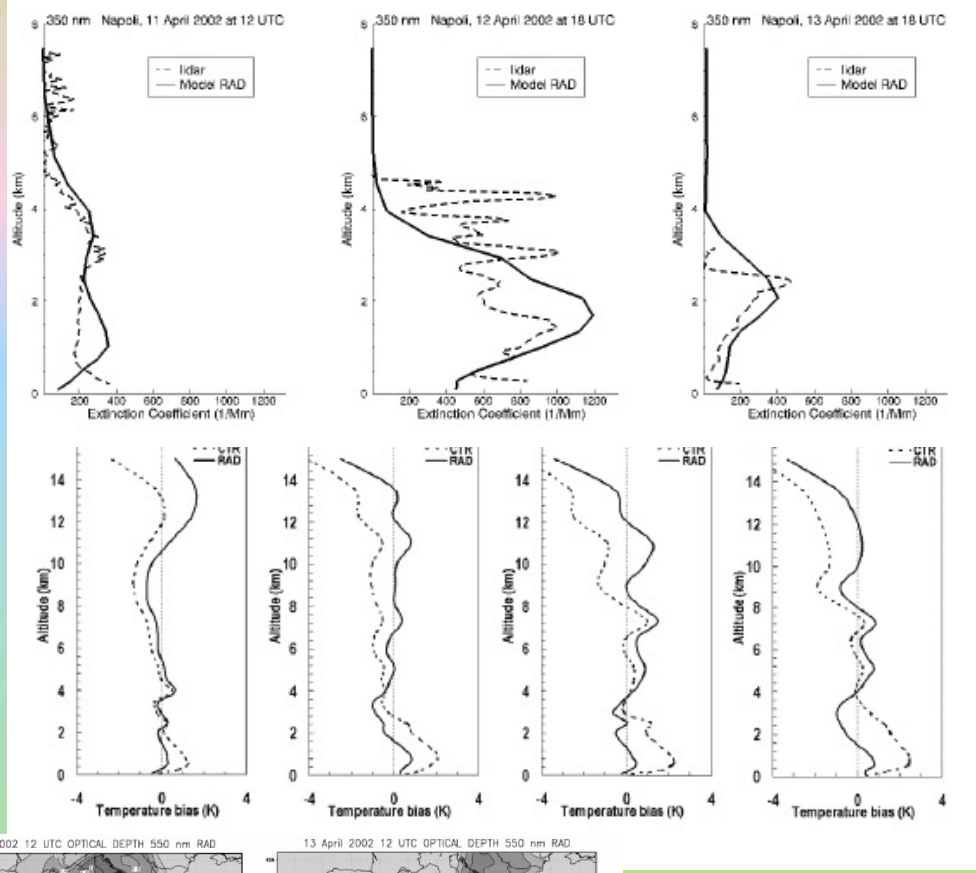

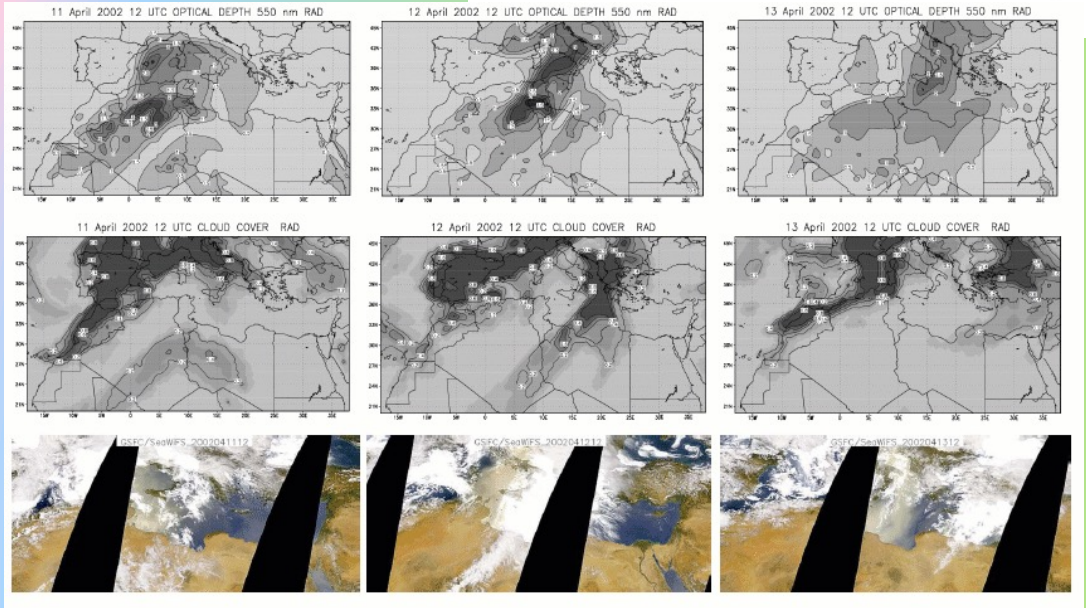

atmosphere – sea interaction
Biogenic sulfate transported by dust

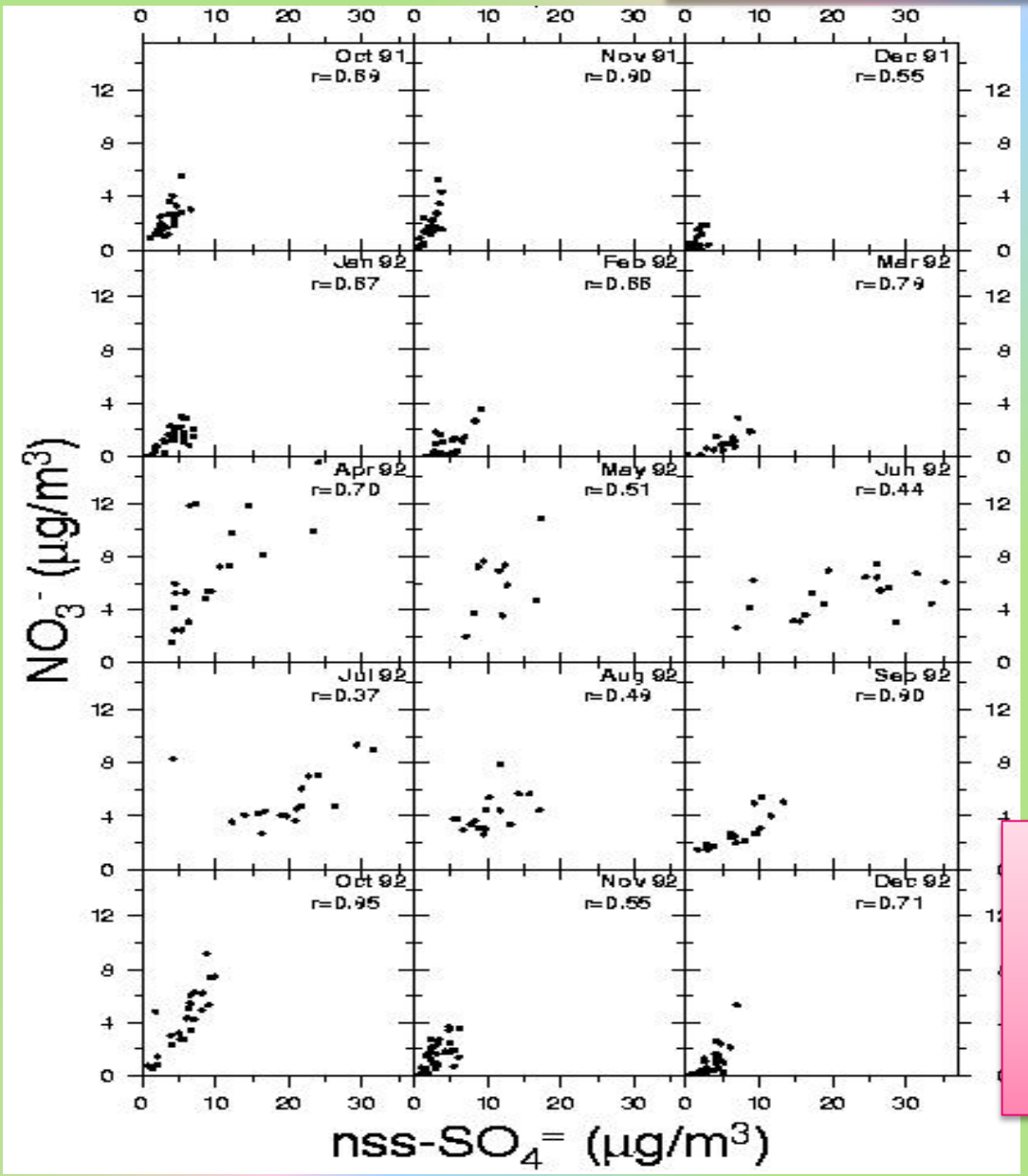

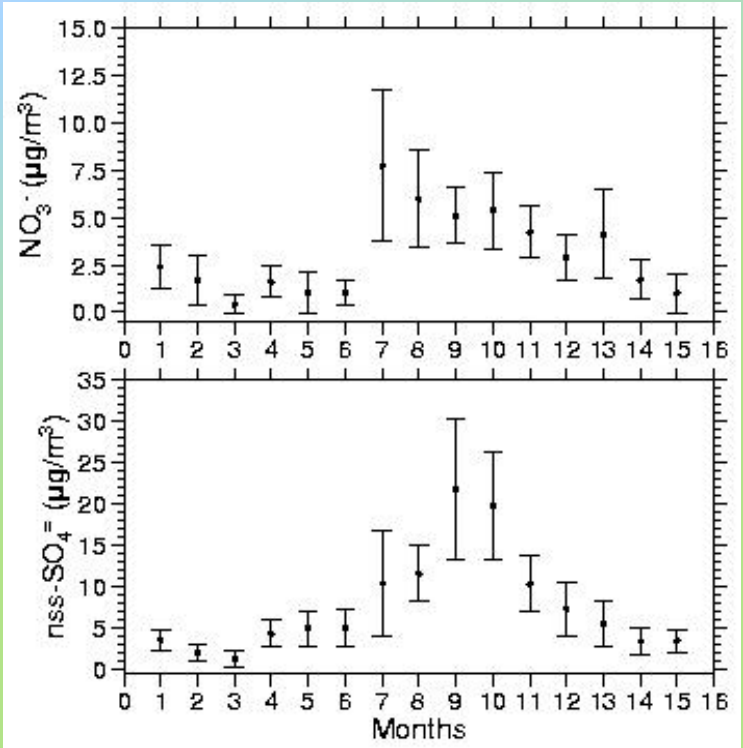

Monthly mean and standard deviation of nitrate and nss-sulfate in aerosols at Erdemli - Özsoy et al. 2000
anthropegenic contribution in summer one outstanding case (27-30 July 1992)

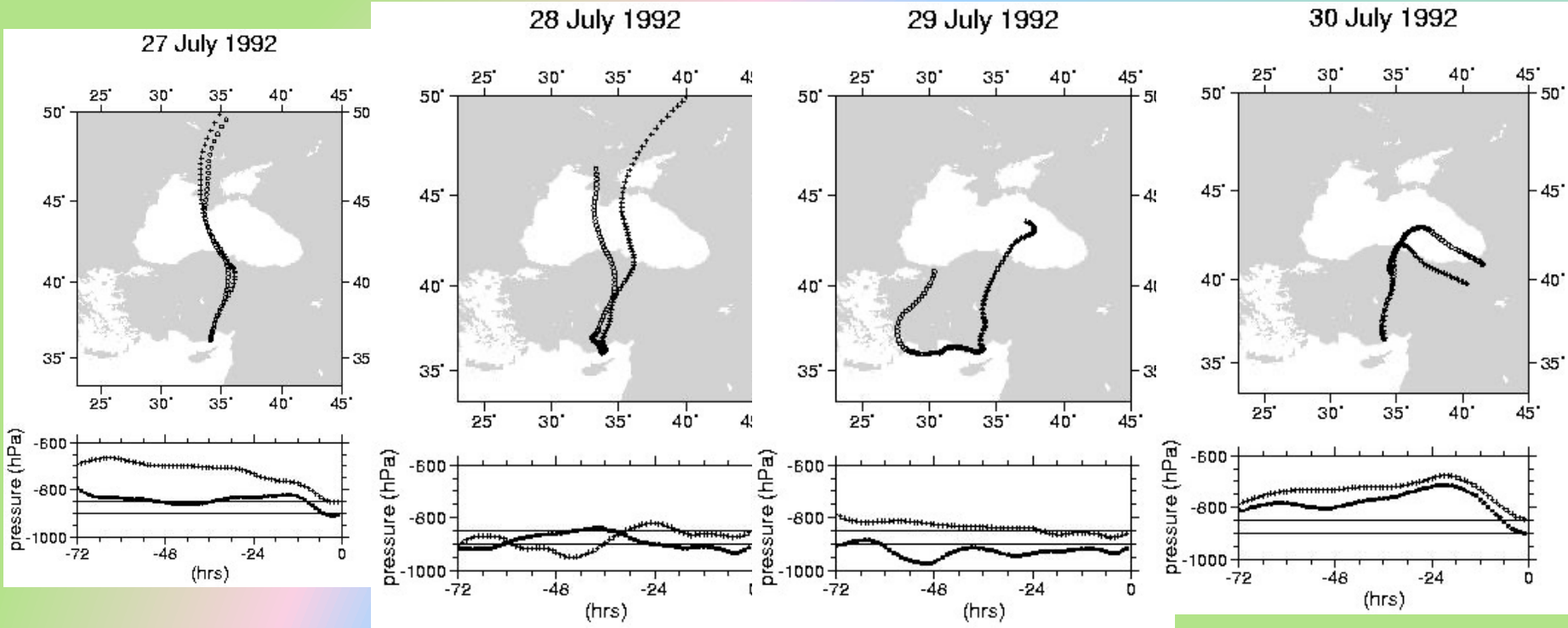

nsss	**29.29**	**31.44**	**4.24**	**21.79**
nitrate	**9.34**	**8.99**	**8.29**	**6.06**

air-mass back trajectories arriving at 900 and 850 hPa levels (a) 27 July 1992; (b) 28 July 1992; (c) 29 July 1992; (d) 30 July 1992 – Özsoy et al. (2000)
aerosol samples sulfate enhanced due to coccolith bloom in the Black Sea

Biogenic sulfur (MSA) from Black Sea Ehux blooms Kubilay et al., 2002

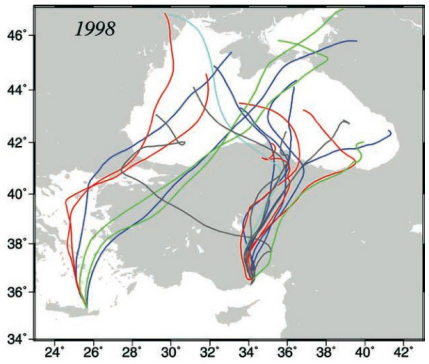

Figure 8. The 3-day air mass back trajectories showing the transport of air masses to the sampling sites at Erdemli and Finokalia from the Black Sea region at selected times during June–July 1998. For Erdemli, blue curves represent the trajectories for 2–6 June, green for 17 June, light blue for 23 June, red for 26–30 June, and black for 1–8 July 1998. For Finokalia, blue curves represent the trajectories for 5–7 June, red for 28–30 June, and green for 22 and 28 July 1998.

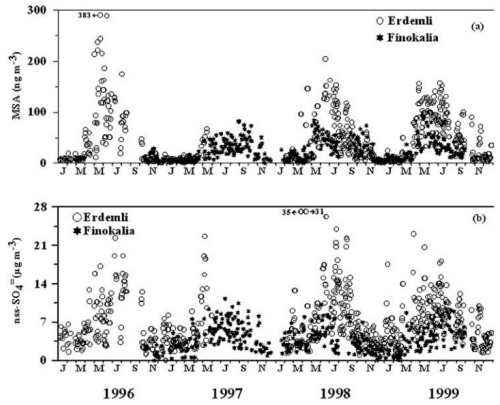

Figure 4. Distributions of (a) aerosol methanesulfonate (MSA in ng m^{-3}) and (b) non-sea-salt (nss) sulfate concentrations (in μg m^{-3}) in samples collected during January 1996 to December 1999 at Erdemli (Turkey) and Finokalia (Crete) shown by open circles and solid stars, respectively.

Bacteria and Fungal colony forming units in aerosol samples collected in Erdemli <effects on ecosystem and human health> Griffin et al., 2007

Fig. 7. Heavy fungal growth on an African desert dust air-sample filter collected on 14 August, 2002 at Erdemli, Turkey. The fungal CFU count on this filter was 239. No bacterial CFU were observed.

Comparison of nutrient inputs to the Sea via atmospheric versus riverine sources: Northern Levantine Basin – Erdemli (Koçak et al., 2010):

- aerosol dry and wet deposition fluxes comparable for phosphate input to the sea
- dissolved silica and ammonia fluxes dominated by wet deposition (~60%)
- dry deposition of nitrate main source (80%) compared to rivers Seyhan and Ceyhan
- DIN and phosphate fluxes dominated by atmospheric inputs (90% and 60%)

Table 7. Comparison of riverine and atmospheric nutrient inputs (10^9 mol km^{-2} yr^{-1}) to the Northeastern Levantine Basin of the Eastern Mediterranean and the literature for the Eastern Mediterranean region.

River	Si_{diss}	PO_4^{3-}	NO_3^-	NH_4^+	DIN	N/P	Si/N
Seyhan	0.620	0.030	0.44	0.08	0.62	18	1.2
Ceyhan	0.730	0.009	0.48	0.09	0.73	65	1.3
Göksu	0.160	0.005	0.08	0.01	0.16	20	1.7
Berdan	0.020	0.001	0.02	0.01	0.02	25	0.8
Lamas	0.010	0.00004	0.01	0.0001	0.01	279	1.1
Winter	0.465	0.014	0.258	0.058	0.366	26	1.3
Transition	0.770	0.020	0.514	0.093	0.604	30	1.3
Summer	0.305	0.010	0.252	0.036	0.242	24	1.3
NLB-R[a]	1.54	0.04	1	0.2	1.2	28	1.3
NLB-A[a]	0.16	0.06	7	3	10	233	0.01
Total[a]	1.70	0.10	8	3.2	11	145	0.1
EMED-A[a]	2.44	0.93	100	47	147	145	0.1
EMED-A[b]	–	0.95	–	–	111	117	–
NLB-R[c]	2.77	0.12	–	–	5.5	46	0.5

[a] Current study, [b] Krom et al., 2004, 2010, [c] Ludwig et al., 2009. NLB: Northeastern Levantine Basin, Total: Riverine + Atmospheric inputs, EMED: Eastern Mediterranean, A: Atmospheric flux and R: Riverine flux.